IOP PUBLISHING PHYSICA SCRIPTA
Phys. Scr. **T129** (2007) 199–204 doi:10.1088/0031-8949/2007/T129/045

Dielectric properties and phase transition of polycrystalline lead zirconate titanate–lead cobalt niobate

Naratip Vittayakorn[1] **and Tawee Tunkasiri**[2]

[1] Materials Science Research Unit, Department of Chemistry, Faculty of Science, King Mongkut's Institute of Technology Ladkrabang, Bangkok 10520, Thailand
[2] Department of Physics, Faculty of Science, Chiang Mai University, Chiang Mai 50200, Thailand

E-mail: naratipcmu@yahoo.com

Received 27 February 2007
Accepted for publication 27 July 2007
Published 28 November 2007
Online at stacks.iop.org/PhysScr/T129/199

Abstract
The binary system of lead zirconate titanate [$Pb(Zr_{1/2}Ti_{1/2})O_3$, PZT] and lead cobalt niobate [$Pb(Co_{1/3}Nb_{2/3}O_3$, PCoN] was fabricated using a high temperature solid state reaction method. The structure and homogeneity of the ceramics obtained have been investigated using x-ray diffraction. The morphology of the ceramics was characterized by scanning electron microscopy (SEM). The results indicated that the presence of PCoN in the solid solution decreases the structural stability of PZT perovskite phase. A transition from tetragonal to pseudo-cubic phase was observed as PCoN increased and the co-existence of tetragonal–pseudo-cubic phases occurred at composition with $x = 0.3$. The permittivity showed a ferroelectric to paraelectric phase transition at 236 °C with a maximum value = 39 000 at 100 Hz at the morphotropic phase boundary (MPB) composition.

PACS numbers: 77.22.−d, 77.80.Bh, 77.84.Dy, 61.10.Nz, 77.80.Dj

(Some figures in this article are in colour only in the electronic version.)

1. Introduction

Lead zirconate titanate (PZT) is a very important material due to its excellent spontaneous polarization. Hence, the ability to produce small actuator components, ultrasonic transducers, hydrophones, speakers, fish finders, sensors, electrical resonators and other devices for microelectronics would be very useful [1, 2]. PZT has an ABO_3 type perovskite structure with the A-site (Pb^{2+}) occupying the cubo-octahedral interstices described by the BO_6-site octahedra. PZT is a solid solution of ferroelectric $PbTiO_3 (T_c = 490\,°C)$ and antiferroelectric $PbZrO_3 (T_c = 230\,°C)$ phases [3]. At room temperature all compositions are ferroelectric when the Zr : Ti ratio < 95 : 5. Above the Curie temperature, the unit cell is cubic, but below, it is distorted to either tetragonal (Zr : Ti < 53 : 47) or rhombohedral (Zr : Ti > 53 : 47). The boundary between these two phases (Zr : Ti ∼ 53 : 47 at room temperature) is known as the morphotropic phase boundary (MPB) [3]. The best piezoelectric and ferroelectric properties can be obtained in PZT near the MPB [4]. Most commercial PZT ceramics are thus designed in the vicinity of the MPB with various doping in order to achieve optimum properties [2, 5]. Recently, many piezoelectric ceramic materials have been developed from binary systems containing a combination of relaxor and normal ferroelectric materials [6] which yield high dielectric permittivities (e.g. PZN–PT [7, 8], PZT–PNN [9]), excellent piezoelectric coefficients (e.g. PZN–PT [7, 8], PZN–PZT [10], PSN–PT [11, 12]) and high pyroelectric coefficients (e.g. PNN–PT–PZ) [13].

Lead cobalt niobate ($Pb(Co_{1/3}Nb_{2/3})O_3$, PCoN) is a typical relaxor ferroelectric characterized by a high dielectric constant, a broad diffuse phase transition near −70 °C and low firing temperature [14]. Though the paraelectric–ferroelectric transition temperature of PCoN is below room temperature, it can be easily shifted upward with the addition of $PbTiO_3$ (PT), which is a normal ferroelectric compound with a phase transition at 490 °C. It was reported that the $Pb(Co_{1/3}Nb_{2/3})O_3$–$PbTiO_3$(PCNT) system had a MPB at about 0.38 mol fraction $PbTiO_3$ and the PCNT ceramics near MPB showed higher Curie temperature

0031-8949/07/129199+06$30.00

($T_c \sim 250\,^\circ$C). So the PCoN-based relaxors are one of the most attractive materials for multilayer ceramic capacitors and electrostrictive actuators [5].

Since PCoN is a relaxor ferroelectric with a broad dielectric peak near $T_c \approx -70\,^\circ$C and PZT (Zr/Ti = 50/50) is a normal ferroelectric with a sharp maximum permittivity at $T_c \sim 390\,^\circ$C, the Curie temperature in the PZT–PCoN system can be engineered over a wide range of temperature by controlling the amount of PCoN in the system. With their complementary characteristics, it is expected that excellent properties can be obtained from ceramics in the PZT–PCoN system. So far, there have been no systematic studies on the structural and dielectric properties of the whole series of PZT–PCoN compositions, which would help in identifying excellent electrical properties within this system. In the present study, PZT and PCoN were chosen as end components to prepare solid solutions via a high temperature solid state reaction method. Structure and morphology are investigated by x-ray diffraction (XRD) analysis and scanning electron microscopy (SEM) respectively. Finally, the dielectric properties of PZT–PCoN ceramics are determined as a function of temperature and frequency to establish structure–property relationships.

2. Experimental

Samples with the composition of $(1-x)\mathrm{Pb(Zr_{0.5}Ti_{0.5})O_3}$–$x\mathrm{Pb(Co_{1/3}Nb_{2/3})O_3}$(PZT–PCoN) with $x = 0$–0.5 were synthesized using the high temperature solid state reaction method. CoO (99.9%), Nb_2O_5 (99.9%), PbO (Fluka, >99% purity) TiO_2 (99.8%) and ZrO_2 (99%) were mixed and milled in ethyl alcohol for 18 h using a ball-mill. In all compositions, 2 mol% excess PbO was added to compensate for lead volatilization during calcination and sintering. After remilling and drying, the mixtures were calcined at 700–950 °C for 4 h in alumina crucible configuration with a heating rate of 20 °C min^{-1}. The calcined powders were milled for 3 h for reduced particle size. After grinding and sieving, the calcined powder was mixed with 5 wt.% poly (vinyl alcohol) binder and uniaxially pressed into a pellet. Binder burnout occurred by slowly heating to 500 °C and holding for 2 h. Sintering occurred between 1100 and 1250 °C with a dwell time of 4 h. To mitigate the effects of lead loss during sintering, the pellets were sintered in a closed alumina crucible containing $PbZrO_3$ powder. The perovskite phase was examined by XRD. Data collection was performed in the 2θ range of 20°–70° using step scanning with a step size of 0.02° and counting time of 2 s step^{-1}.

After surface grinding, the samples were electroded using sputtered gold and air-dried silver paint was applied. The relative permittivity (ε_r) and dissipation factor (tan δ) were measured using an automated measurement system. This system consisted of an LCR meter (HP-4284A, Hewlett-Packard Inc.) in connection with a sample holder (Norwegian Electroceramics) capable of high temperature measurement. The capacitance and dissipation factors of each sample were measured at 100 Hz, 1, 10 and 100 kHz and temperature varied between 25 and 400 °C. A heating rate of 2 °C min^{-1} was used during measurements. The dielectric constant is then calculated from $\varepsilon_r = Cd/\varepsilon_o A$, where C is the capacitance of the sample, d and A are the thickness and the area of the electrode, respectively, and ε_o is the dielectric permittivity of vacuum (8.854×10^{-12} F m^{-1}).

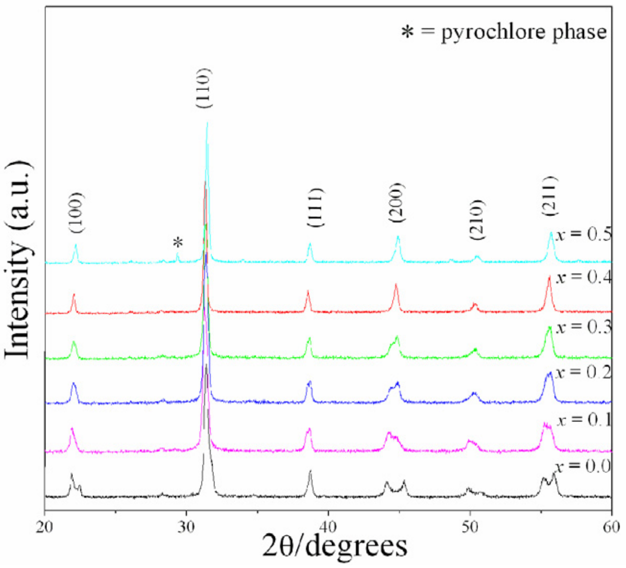

Figure 1. XRD patterns of PZT–PCoN ceramics.

3. Result and discussion

3.1. Crystal structure and microstructure

The XRD patterns of $(1-x)$PZT–xPCoN ceramics with various x values are shown in figure 1. The patterns show single-phase perovskite-structured ceramics with $x \leqslant 0.4$. Evidence for the pyrochlore or other second phases was not detected in the patterns. Pyrochlore peaks, identified by '*' in figure 1, were found in the samples with $x = 0.5$. These results indicated that the presence of PCoN in the solid solution decreases the structural stability of PZT perovskite phase by its tolerance factor and electronegativity [15]. Figure 2(A) shows a SEM micrograph of the polished surface of the sintered pellet sample. The ceramic has a close microstructure with low porosity, and the packed grains are in the size range of 1–4 μm. It was found from the SEM micrograph that grains of different sizes are homogeneously distributed over the entire surface of the sample, and hence the sample is highly dense. It should be noted that a rectangular shape of $Pb_3Nb_4O_{13}$ or octahedral shape of pyrochlore phase has been reported inside and on the surface of the composition $x = 0.5$ as shown in figure 2(B).

The $PbZrO_3$–$PbTiO_3$ phase diagram predicts that at room temperature $\mathrm{Pb(Zr_{1/2}Ti_{1/2})O_3}$ falls within the tetragonal phase field near the MPB. The crystal symmetry for pure PCoN is cubic at room temperature. Below $T_{max} \approx -70\,^\circ$C, the symmetry changes to rhombohedral. Therefore, with increasing x the crystal symmetry should change due to the effects of the increased PCoN fraction and the decrease in T_C. It is well known that in the pseudo-cubic phase, the profile will show a single narrow peak because all the planes of {2 0 0} share the same lattice parameters, while in the tetragonal phase, the {2 0 0} profile should be split into two peaks with the intensity height of the former being half of the

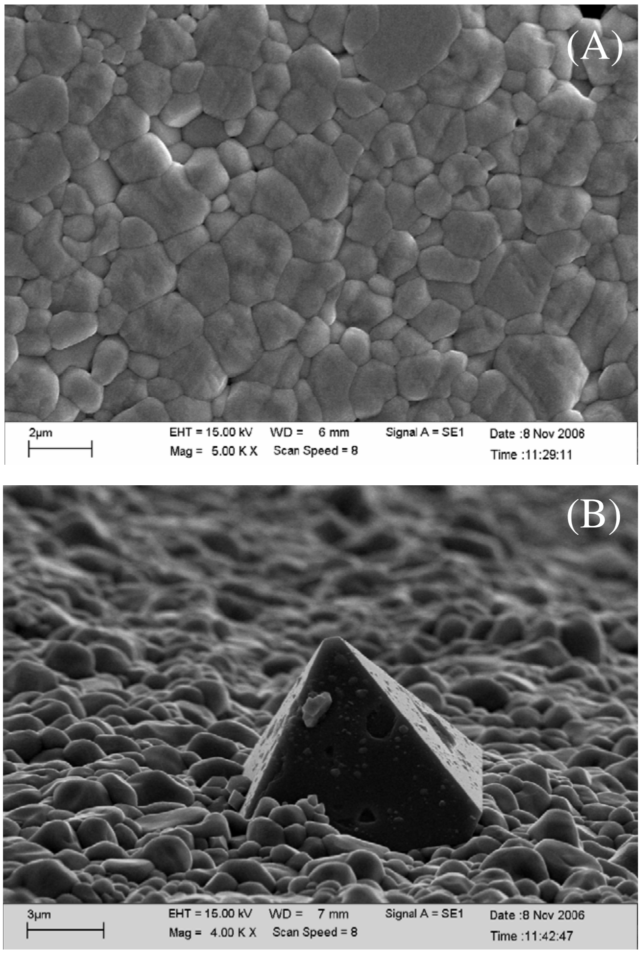

Figure 2. SEM microstructures of the surfaces of composition (A) $x = 0.1$ and (B) $x = 0.5$.

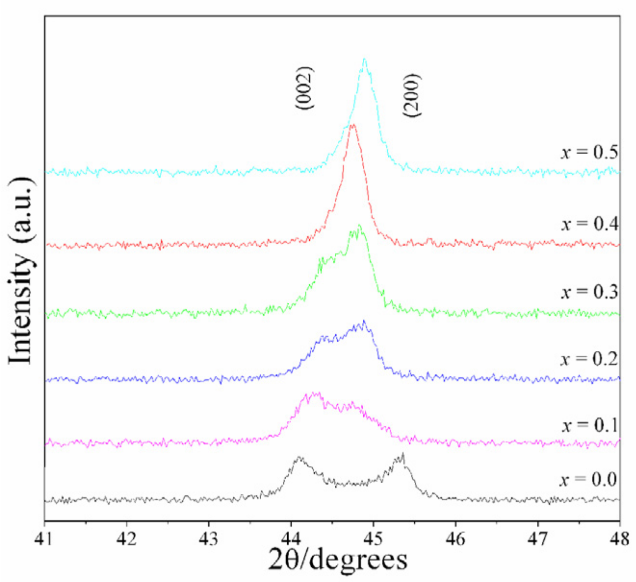

Figure 3. XRD pattern of the (2 0 0) peak of $(1-x)$PZT$-x$PCoN, $x = 0.0$–0.1 ceramics.

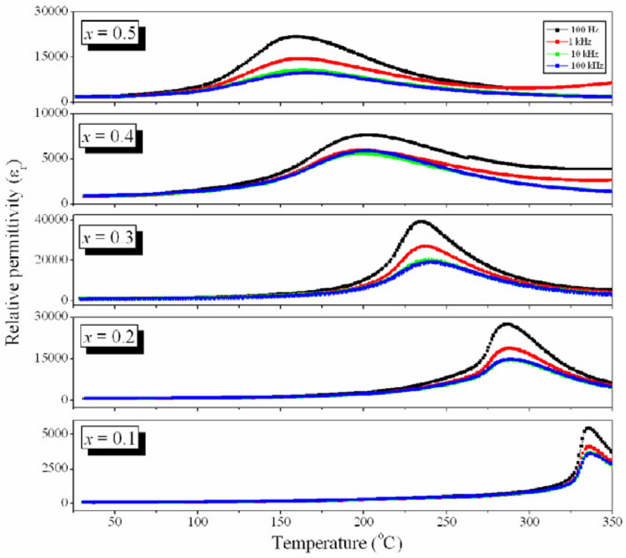

Figure 4. Dielectric properties as a function of temperature at frequencies between 100 Hz and 100 kHz.

latter because the lattice parameters of (2 0 0) and (0 2 0) are the same but are slightly different from those of (0 0 2). Figure 3 shows the evolution of the (2 0 0) peak as a function of composition. At low PCoN concentration, the XRD pattern shows strong (2 0 0) peak splitting which is indicative of the tetragonal symmetry. As the PCoN concentration increased, the (2 0 0) transformed to a single peak which suggests pseudo-cubic symmetry. The results show that the mixed phase region of the coexisting ferroelectric tetragonal and ferroelectric pseudo-cubic phases is located in the composition $x = 0.3$ of the $(1-x)$PZT–xPCoN binary system. A transition from tetragonal to pseudo-cubic phase was observed as PCoN increases. It is interesting to note that the influence of the addition of $Pb(Co_{1/3}Nb_{2/3})O_3$ on the phase transition of the $Pb(Zr_{1/2}Ti_{1/2})O_3$ system is similar to that of the $Pb(Zr_{1/2}Ti_{1/2})O_3$–$Pb(Ni_{1/3}Nb_{2/3})O_3$ and $Pb(Zr_{1/2}Ti_{1/2})O_3$–$Pb(Zn_{1/3}Nb_{2/3})O_3$ systems [9, 16, 17].

3.2. Dielectric properties

The characteristic temperature and frequency dependence of the relative permittivity for $(1-x)$PZT–xPCoN, $x = 0.1$–0.5 is shown in figure 4. With increasing concentration of PCoN, the dielectric constant tends to increase. The effect of increasing dielectric constant at room temperature with increasing PCoN content is interpreted to be due to the possibility of the decrease of the transition temperature to near room temperature. The dielectric properties of PZT ceramic change significantly with temperature, but are nearly independent of frequency, except in the vicinity of the phase transformation temperature [18, 19]. This is a typical characteristic of ferroelectric ceramics with a long-range ordered structure. The Curie temperature (T_C) for PZT ceramic is not determined in this study as a result of limited range of the measuring set-up, though it is widely known to be close to 400 °C [18, 19]. While PZT exhibits normal ferroelectric behaviour, PCoN is a relaxor ferroelectric material as a result of short-range ordered structure with nanometer scale heterogeneity in composition [20].

The nature of the homogeneously polarized states is believed to be primarily controlled by the concentration of PCoN. When PCoN is added to form the binary system

Table 1. Characteristics of $(1-x)$PZT–xPCoN ceramics with optimized processing conditions.

Composition x	Crystal structure	T_m (°C)	Relative permittivity at 25 °C	Relative permittivity at T_{max}	$\tan\theta$ at 25 °C	$\tan\theta$ at T_m	δ
0.1	T	336	350	5500	0.042	0.024	10.1
0.2	T	288	580	27 500	0.042	0.018	32.4
0.3	PC + T	136	875	39 500	0.029	0.025	33.9
0.4	PC	199	1250	7700	0.011	0.047	48.6
0.5	PC	161	1900	22 000	0.005	0.182	49.6

PC = Pseudo-cubic, T = tetragonal.

with PZT, a clear shift of the transition temperature to lower temperatures was observed. In addition, the dielectric maximum decreased as the x value increased. Moreover the dielectric peak became broader as the PCoN content increased. It is interesting to note that all compositions show dispersive dielectric behaviour with respect to frequency. However, the frequency dispersion in the PZT–PCoN binary system is not as strong as that in the pure relaxor PCoN. A smooth transition from normal to relaxor ferroelectric behaviour is observed with increasing mole percent of PZT from $x = 0.1$ to 0.5. This transition is characterized by the enhancement of the first-order nature of the phase transformation and the diminishment of the relaxor behaviour (i.e. the permittivity dispersion) over the broad temperature range in the vicinity of T_{max}. Similar phenomena have been observed in PZT–PZN [16, 17], PZT–PNN [9] and PZT–PMN [19]. For all compositions, table 1 lists the temperature at which the permittivity is maximum (T_{max}), and the relative permittivity both at room temperature and at T_{max}. It is also evident from figure 4 and table 1 that 0.7 PZT–0.3 PZN composition exhibited a maximum permittivity of approximately 39 000 (at 1 kHz) with a $T_{max} \sim 236$ °C. Combined with the XRD examination described in section 3.1, the anomaly in dielectric properties clearly indicates a phase transformation over that compositional range. Therefore, an MPB separating the tetragonal phase (PZT-rich) from the pseudo-cubic phase (PCoN-rich) exists at the composition $x = 0.3$.

It should also be noted here that the PCoN-rich samples show very strong frequency-dependent dielectric dispersion significantly at high temperature ($T > T_{max}$) as a result of thermally activated space charge conduction. In general, lead-based ceramic is known to have a significant concentration of oxygen vacancies due to super-oxidation, where there exists an excess of Pb-vacancies due to the lead oxide volatility over oxygen vacancies [3]. This results in the generation of space-charge fields which stabilize the domain structure [21]. However this behaviour may be caused by the valence variation between Co^{2+} and Co^{3+}. The conduction resulting from the addition of PCN can be understood from the charge hopping mechanism common among transition metal ions. These ions, such as Fe, Ni, or Co, can assume different charge states more readily than other cations: when Co enters the perovskite lattice as a 2^+ cation, it can undergo a local thermodynamic reaction through $Co^{2+} = Co^{3+} + e^-$. The electron is mostly likely attached to the Co^{3+} cations, but the transfer of the electronic charge from one cation to another through the lattice results in charge conduction. This charge transfer process corresponds to a low mobility and is similar to the small polaron mechanism [22]. The maximum permittivity $\varepsilon_{r,max}$ and T_{max} as a function of the mole fraction of PCoN (x) are represented in figure 5. There is a good linear relationship between T_{max} and x, indicating that this system is a well behaved complete solid solution. The T_{max} of the constituent compounds PCoN and PZT are −70 and 390 °C, respectively, which can be used to calculate an empirical estimate of T_{max} via the equation:

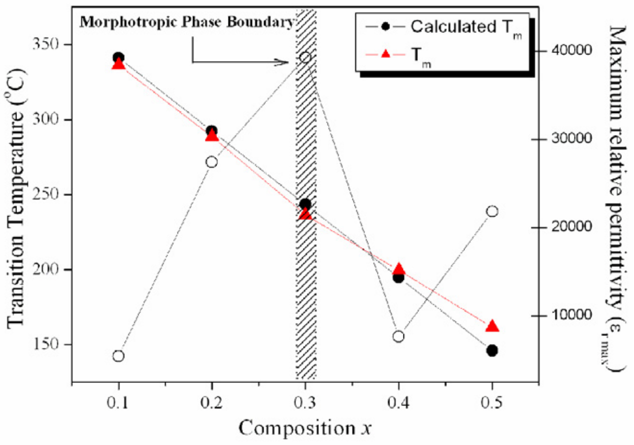

Figure 5. Transition temperatures (T_m), calculated T_m and maximum relative permittivity ($\varepsilon_{r,max}$) as a function of composition x.

$$T_{max} = x(390\,^{\circ}\mathrm{C}) + (1-x)(-120\,^{\circ}\mathrm{C}) \qquad (1)$$

The variation of the measured T_{max}, the calculated T_{max}, and the measured $\varepsilon_{r,max}$ as a function of composition x is shown in figure 6. The highest $\varepsilon_{r,max}$ of 39 000 at 236 °C at 10 kHz was observed for the composition at the MPB 0.7 PZT–0.3 PCoN. It is evident from the data that equation (1) gives a reasonable approximation of the transition temperature T_{max}. This result suggests that the transition temperature of the $(1-x)$PZT–xPCoN system can be varied over a wide range from –70 to 390 °C by controlling the amount of PCoN in the system.

It is generally accepted that a relaxor ferroelectric can be described by a simple quadratic law. This arises from the fact that the total number of relaxors contributing to the permittivity response in the vicinity of the permittivity peak is temperature-dependent, and the temperature distribution of this number is given by a Gaussian function about a mean value T_o with a standard deviation σ. The diffusiveness parameter (δ) of the transition was calculated from the

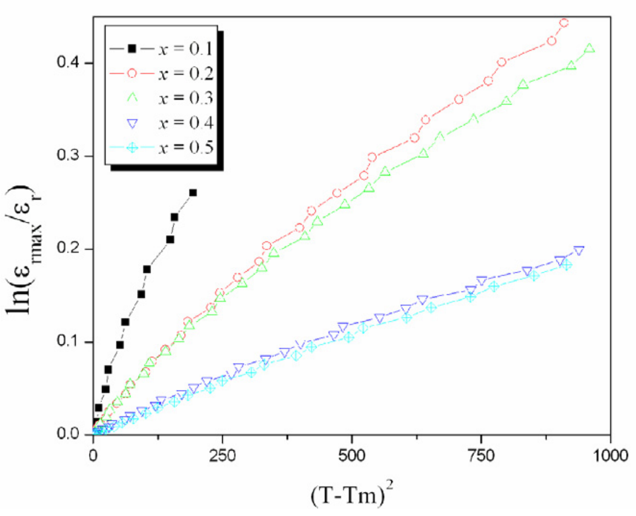

Figure 6. Quadratic dependence of temperature on logarithmic dielectric constant of PZT–PCoN ceramic as a function of composition *x*.

expression (23):

$$\frac{K_m}{K(f, T)} = \exp\left(\frac{(T - T_m(f))^2}{2\delta^2}\right) \qquad (2)$$

where K_m is the maximum value of the dielectric constant at $T = T_m(f)$ and $K(f, T)$ is the intrinsic dielectric constant of the sample. If ln (K_m/K_g) is plotted versus $(T - T_m)^2$, the slope of the fitted curve, $1/(2\delta^2)$, will give the value of the diffuseness parameter. As clarified by Pilgrim *et al* [23], the estimate of δ is valid for the range of $K_m/K(f, T) < 1.5$. Figures 3(a) and (b) display the curves of ln $(K_m/K(f, T))$ versus $(T - T_m)^2$ under the condition $K_m/K(f, T) < 1.5$. The diffuseness parameter increased significantly with PCoN substitution. A similar trend was also observed for substitution with alkali-earth metals in lead-based perovskites [24–27]. The parameter δ can be used to measure the degree of diffuseness of the phase transition in mixed normal–relaxor ferroelectric materials. The lower δ value in the PZT-rich samples indicates that the homogeneity at the atomic scale is much higher than in PCoN-rich samples. As the PCoN mole fraction increases, the solid solution displays more diffuse phase transition characteristics.

4. Conclusions

The $(1 - x)\text{Pb}(\text{Zr}_{1/2}\text{Ti}_{1/2})\text{O}_3$–$(x)\text{Pb}(\text{Co}_{1/3}\text{Nb}_{2/3})\text{O}_3$ (where $x = 0$, 0.1, 0.2, 0.3, 0.4 and 0.5) ceramic composites are prepared using a high temperature solid state reaction method. The dielectric properties of the ceramics are determined as functions of both temperature and frequency with an automated dielectric measurement system. Dielectric measurements are taken over the temperature range of 25–400 °C with measuring frequency between 100 Hz and 100 kHz. The results indicate that the dielectric properties of the binary system PZT–PCoN follow normal and relaxor ferroelectric behaviour. Dielectric behaviour of the 0.9 PZT–0.1 PCoN ceramics is more like normal ferroelectrics, while the other compositions are obviously of diffuse phase transition. It is also observed that the transition temperature decreases and the maximum dielectric constant increases with increasing amount of PCoN in the system. Investigations on the structure and properties of the PZT–PCoN system over the range $x = 0.1$–0.5 reveal an MPB at $x = 0.3$, separating tetragonal phase from pseudo-cubic phase. Examination of the dielectric spectra indicates that PZT–PCoN exhibits an extremely high relative permittivity at the MPB composition. The permittivity shows a ferroelectric to paraelectric phase transition at 236 °C with a maximum value = 39 000 at 100 Hz at the MPB composition.

Acknowledgments

This work was supported by the Thailand Research Fund (TRF), the Commission on Higher Education (CHE), Office of the National Research Council of Thailand (NRCT) and King Mongkut's Institute of Technology Ladkrabang (KMITL).

References

[1] Haertling G H 1999 Ferroelectric ceramics: history and technology *J. Am. Ceram. Soc.* **82** 797–818
[2] Uchino K 2000 *Ferroelectric Devices* (New York: Dekker)
[3] Jaffe B and Cook W R 1971 *Piezoelectric Ceramic* (Marietta, OH: R.A.N. Publishers)
[4] Bhalla A S, Guo R and Roy R 2000 The perovskite structure—a review of its role in ceramic science and technology. *Mater. Res. Innovat.* **4** 3
[5] Xu Y 1991 *Ferroelectric Materials and Their Application* (Amsterdam: Elsevier)
[6] Park S-E and Shrout T R 1997 Characteristics of relaxor-based piezoelectric single crystals for untrasonic transducers *IEEE Trans. UFFC* **44** 1140
[7] Kuwata J, Uchino K and Nomura S 1981 Phase transition in the PZN–PT system *Ferroelectrics* **37** 579
[8] Mulvihill M L, Cross L E, Cao W and Uchino K 1997 Domain-related phase transitionlike behavior in lead zinc niobate relaxor ferroelectric single crystals *J. Am. Ceram. Soc.* **80** 1462
[9] Vittayakorn N, Rujijanagul G, Tan X, Marquardt M A and Cann D P 2004 The morphotropic phase boundary and dielectric properties of the $x\text{Pb}(\text{Zr}_{1/2}\text{Ti}_{1/2})\text{O}_3$–$(1 - x)\text{Pb}(\text{Ni}_{1/3}\text{Nb}_{2/3})\text{O}_3$ perovskite solid solution *J. Appl. Phys.* **96** 5103
[10] Fan H and Kim H-E 2002 Preparation and improvement in the electrical properties of lead-zinc-niobate-based ceramics by thermal treatments *J. Mater. Res.* **17** 180
[11] Furukawn O, Yamashita Y, Harata M, Takahashi T and Inagai K 1985 *Japan. J. Appl. Phys.* **24** 96
[12] Tennery V J, Hang K W and Novak R E 1968 Ferroelectric and structure properties of the PSNT system *J. Am. Ceram. Soc.* **51** 671–4.
[13] Luff D, Lane R, Brown K R and Marshallsay H J 1974 Ferroelectric ceramic with high pyroelectric properties. *Trans. J. Br. Ceramic Soc.* **73** 251
[14] Smolenskii G A and Agranovskaya A L 1958 Dielectric polarization of and losses of some complex compounds *Sov. Phys.–Tech. Phys.* 1380
[15] Shrout T R and Halliyal A 1987 Proparation of lead-based ferroelectric relaxors for capacitors *Am. Ceram. Soc. Bull.* **66** 704
[16] Vittayakorn N, Puchmark C, Rujijanagul G, Tan X and Cann D P 2006 Piezoelectric properties of $(1- x)\text{Pb}(\text{Zr}_{1/2}\text{Ti}_{1/2})\text{O}_3$–$x\text{Pb}(\text{Zn}_{1/3}\text{Nb}_{2/3})\text{O}_3$ ceramics prepared by the columbite-(wolframite) precursor method *Curr. Appl. Phys.* **6** 303–6

[17] Vittayakorn N, Rujijanagul G, Tan X, He H, Marquardt M A and Cann D P 2006 Dielectric properties and morphotropic phase boundary in the xPb($Zn_{1/3}Nb_{2/3}$)O_3–(1−x)Pb ($Zr_{0.5}Ti_{0.5}$)O_3 pseudo-binary system *J. Electroceram.* **16** 141–9

[18] Koval V, Alemany C, Brianin J and Bruncková H 2004 Dielectric properties and phase transition behaviour of xPMN–(1−x)PZT ceramic systems *J. Electroceram.* **10** 19–29

[19] Yimnirun R, Ananta S and Laoratanakul P 2005 Dielectric and ferroelectric properties of lead magnesium niobate–lead zirconate titanate ceramics prepared by mixed-oxide method *J. Eur. Ceram. Soc.* **25** 3235–42

[20] Randall C A, Bhalla A S, Shrout T R and Cross L E 1990 Relationship between B-site order and properties in Pb(B′B″)O_3 perovskites *Ferroelectrics* **11** 103

[21] Takahashi M 1970 Space charge effect in lead zirconate titanate ceramics caused by the addition of impurities *Japan. J. Appl. Phys.* **9** 1236

[22] Goulding R H, Zinkle S J, Rasmussen D A and Stoller R E 1996 Transient effects of ionising and displacive radiation on the dielectric properties of the ceramics *J. Appl. Phys.* **79** 2920

[23] Pilgrim S M, Sutherland A E and Winzer S R 1990 Diffuseness as a useful parameter for relaxor ceramics *J. Am. Ceram. Soc.* **73** 3122

[24] Yao W, Feng C, Li H, Yang Y and Yu Y 2003 Dielectric properties and dielectric aging of 0.9PMN–0.1PT doped with CaO *Mater. Lett.* **57** 2834

[25] Ahn B-Y and Kim N-K 2000 Effects of barium substitution on perovskite formation, dielectric properties, and diffuseness characteristics of lead zinc niobate ceramics *J. Am. Ceram. Soc.* **83** 1720–26

[26] Butcher S J and Thomas N W 1991 Ferroelectricity in the $Pb_{1-x}Ba_x(Mg_{1/3}Nb_{2/3})O_3$ *J. Phys. Chem. Solids.* **52** 595

[27] Vittayakorn N, Uttiya S, Rujijanagul G and Cann D P 2005 Dielectric and ferroelectric characteristics of 0.7 PZT–0.3 PZN ceramics substituted with Sr *J. Phys. D: Appl. Phys.* **38** 2942–6

Japanese Journal of Applied Physics
Vol. 47, No. 2, 2008, pp. 998–1002

Synthesis and Dielectric and Ferroelectric Properties of Ceramics in $(1-x)\mathrm{Pb(Zr_{1/2}Ti_{1/2})O_3}$–$(x)\mathrm{Pb(Co_{1/3}Nb_{2/3})O_3}$ System

Anurak PRASATKHETRAGARN*, Naratip VITTAYAKORN[1],
Supon ANANTA, Rattikorn YIMNIRUN, and David P. CANN[2]

Department of Physics, Faculty of Science, Chiang Mai University, Chiang Mai 50200, Thailand
[1]*Department of Chemistry, Faculty of Science, King Mongkut's Institute of Technology Ladkrabang, Bangkok 10520, Thailand*
[2]*Materials Science, Department of Mechanical Engineering, Oregon State University, Corvallis, OR 97331, U.S.A.*

(Received August 16, 2007; revised September 28, 2007; accepted October 26, 2007; published online February 15, 2008)

Ceramics in a PZT–PCN system with the formula $(1-x)\mathrm{Pb(Zr_{1/2}Ti_{1/2})O_3}$–$(x)\mathrm{Pb(Co_{1/3}Nb_{2/3})O_3}$, where $x = 0.1$–0.5, were prepared using a solid-state mixed-oxide technique (the columbite-wolframite precursor method). The phase formation behavior and microstructure were studied using X-ray diffraction (XRD) analysis and scanning electron microscopy (SEM), respectively. The dielectric and ferroelectric properties of the compounds were studied and discussed. Phase-pure perovskites of PZT–PCN ceramics were obtained over a wide compositional range. In addition, the XRD, dielectric, and ferroelectric properties confirmed that the morphotropic phase boundary (MPB) composition between the tetragonal and pseudo cubic phases of this system lied between $0.2 \leq x \leq 0.3$. [DOI: 10.1143/JJAP.47.998]

KEYWORDS: ferroelectric properties, perovskites, MPB, phase transition

1. Introduction

Lead-based perovskite-type solid solutions consisting of ferroelectric and relaxor materials have attracted more and more fundamental and practical attention because of their excellent dielectric, piezoelectric, and electrostrictive properties, which are useful in actuating and sensing applications.[1] Recently, many piezoelectric ceramic materials have been developed from binary systems containing a combination of relaxor and normal ferroelectric materials[2] that yield high dielectric permittivities [e.g., $\mathrm{Pb(Zn_{1/3}Nb_{2/3})O_3}$–$\mathrm{PbTiO_3}$ (PZN–PT)[3,4] and $\mathrm{Pb(Zr_{1/2}Ti_{1/2})O_3}$–$\mathrm{Pb(Ni_{1/3}Nb_{2/3})O_3}$ (PZT–PNN)[5]], excellent piezoelectric coefficients [e.g., $\mathrm{Pb(Zn_{1/3}Nb_{2/3})O_3}$–$\mathrm{PbTiO_3}$ (PZN–PT),[3,4] $\mathrm{Pb(Zr_{1/2}Ti_{1/2})O_3}$–$\mathrm{Pb(Zn_{1/3}Nb_{2/3})O_3}$ (PZN–PZT),[6] and $\mathrm{Pb(Sc_{1/3}Nb_{2/3})O_3}$–$\mathrm{PbTiO_3}$ (PSN–PT)[7,8]], and high pyroelectric coefficients [e.g., $\mathrm{Pb(Ni_{1/3}Nb_{2/3})O_3}$–$\mathrm{PbTiO_3}$–$\mathrm{PbZrO_3}$ (PNN–PT–PZ)[9]]. Of the lead-based complex perovskites, lead zirconate titanate [$\mathrm{Pb(Zr_{1/2}Ti_{1/2})O_3}$ or PZT] ceramics have been investigated from both fundamental and applied viewpoints.[10] A solid solution of $\mathrm{Pb(Zr_{1-x}Ti_x)O_3}$ (PZT) was found to host exceptionally high value for dielectric and piezoelectric properties for compositions close to the morphotropic phase boundary (MPB). This MPB is located at a $\mathrm{PbTiO_3{:}PbZrO_3}$ of $\sim 1:1$ and separates the Ti-rich tetragonal phase from the Zr-rich rhombohedral phase.[10] Furthermore, it has a high T_C of 390 °C, which allows piezoelectric devices to be operated at relatively high temperatures. Most commercial PZT ceramics are designed in the vicinity of the MPB with various doping methods in order to achieve high properties.

Lead cobalt niobate (PCN) is a perovskite relaxor ferroelectric with a broad diffuse phase transition near −70 °C.[11] The structure is cubic at room temperature (RT). In this compound, the octahedral sites of the crystal are randomly occupied by $\mathrm{Co^{2+}}$ and $\mathrm{Nb^{5+}}$ ions.[12] Malkov and Venevtsev have indicated that there are large deviations in the temperatures at which the permittivity is maximum (T_m) for single-crystal and ceramic samples.[13] The effects of the DC bias on the dielectric properties have been reported as a function of temperature for single-crystal $\mathrm{Pb(Co_{1/3}Nb_{2/3})O_3}$ with a diffuse phase transition.[14] Although the paraelectric–ferroelectric transition temperature of PCN is below RT, it can be easily shifted upward with the addition of $\mathrm{PbTiO_3}$ (PT), which is a normal ferroelectric compound with a phase transition at 490 °C.[15] In addition, it is well known that the addition of PZT enhances the piezoelectric, dielectric, and ferroelectric properties in a solid solution with a relaxor ferroelectric such as PZT–PZN,[16,17] PZT–PNN,[5] and PZT–PMN.[18] On the basis of this approach, solid solutions of PZT and PCN are expected to synergistically combine the properties of both the normal ferroelectric PZT and relaxor ferroelectric PCN, which could exhibit piezoelectric and dielectric properties that are better than those of the single-phase PZT and PCN.[12,19] There have been no systematic studies on the electrical properties of ceramics within a wide composition range between PZT and PCN.

The overall purpose of this study is to determine the phase transition, grain size, and composition dependence of the dielectric properties and ferroelectric behavior of ceramics in a $(1-x)\mathrm{Pb(Zr_{1/2}Ti_{1/2})O_3}$–$(x)\mathrm{Pb(Co_{1/3}Nb_{2/3})O_3}$ (where $x = 0.1$–0.5) binary system prepared using the columbite-wolframite precursor method.

2. Experimental Procedure

Reagent-grade oxides of PbO, CoO, $\mathrm{Nb_2O_5}$, $\mathrm{ZrO_2}$, and $\mathrm{TiO_2}$ (anatase-structure) were used as raw materials. The columbite $\mathrm{CoNb_2O_6}$ and wolframite $\mathrm{ZrTiO_4}$ precursors were weighed and introduced into the batch calculations. $\mathrm{CoNb_2O_6}$ and $\mathrm{ZrTiO_4}$ powders were prepared at calcination temperatures of 1100 and 1450 °C for 2 h, respectively. In the present work, $(1-x)\mathrm{Pb(Zr_{1/2}Ti_{1/2})O_3}$–$(x)\mathrm{Pb(Co_{1/3}Nb_{2/3})O_3}$ samples with compositions of $x = 0.1$–0.5 were prepared from $\mathrm{ZrTiO_4}$, $\mathrm{CoNb_2O_6}$, and PbO powders. PZT–PCN powders were synthesized using the solid-state reaction of these raw materials and mixed by a vibro-milling technique in ethanol for 1 h. PbO excess of 2.0 mol % was constantly added to compensate for lead losses during calcination and sintering.[17] After drying, the product was calcined in an alumina crucible at a temperature of 950 °C.

---

*E-mail address: Prasatkhetragarn@yahoo.com

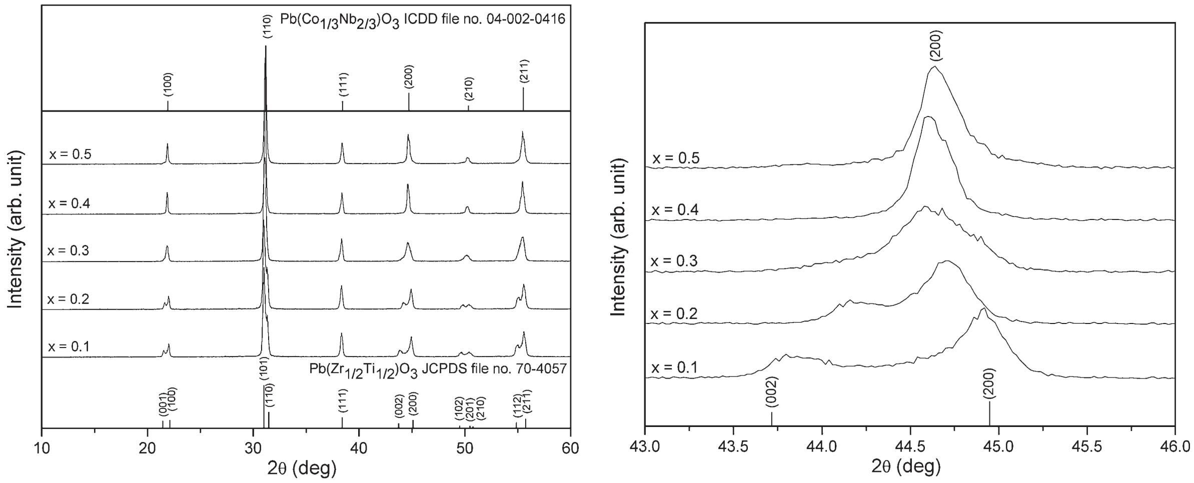

(a) (b)

Fig. 1. XRD patterns of $(1-x)$PZT–(x)PCN ceramics, where $x = 0.1$–0.5.

The calcined powders were pressed hydraulically to form disc-shaped pellets with a diameter of 10 mm and a thickness of 1 mm, with 1 wt % poly(vinyl alcohol) (PVA) added as a binder. The pellets were sintered at 1200 °C for 2 h at a heating/cooling rate of 5 °C/min. The phase structure of the powders was analyzed via X-ray diffraction (XRD; Siemens-D500 diffractometer) analysis using Cu Kα radiation. The microstructures of the sintered samples were examined using scanning electron microscopy (SEM; JEOL JSM-840A). The dielectric properties of the samples were measured using an automated measurement system. This system consisted of an LCR meter (Hewlett-Packard HP-4284A) in connection with a Delta Design 9023 temperature chamber and a sample holder (Norwegian Electroceramics) capable of high-temperature measurement. The ferroelectric properties were examined using a simple Sawyer–Tower circuit.[18)]

3. Results and Discussion

The XRD patterns of $(1-x)$PZT–(x)PCN ceramics with various x values are shown in Fig. 1. It can be seen that a complete crystalline solution of the perovskite structure is formed throughout the entire compositional range without the presence of pyrochlore or unwanted phases. From the XRD data, the $Pb(Zr_{1/2}Ti_{1/2})O_3$ ceramic is identified as a single-phase material with a perovskite structure having tetragonal symmetry, which was matched with JCPDS file no. 70-4057. The XRD patterns of the PZT–PCN compositions show a range in symmetry between the tetragonal and pseudo cubic perovskite types.[20)] For a better comparison, ICDD file no. 04-002-0416 for $Pb(Co_{1/3}Nb_{2/3})O_3$ with pseudo cubic structural symmetry is also displayed in Fig. 1. It is clear that the crystal symmetry should change owing to the effects of increasing the PCN fraction and a corresponding decrease in T_C. It is well known that in the pseudo cubic phase, the (200) profile will show a single narrow peak, while in the tetragonal phase, the (200) profile should be split into two peaks. More interestingly, the composition at $x = 0.3$ exhibited peak broadening at a 2θ of ~44–45°, indicating the structural transformation from the tetragonal phase, characterized by the shifting of the (002)/(200) peaks to the pseudo cubic phase. This observation is obviously associated with the composition showing the coexistence of two symmetries, which in this case are the tetragonal and pseudo cubic phases. To a first approximation, it could be said that the composition with $x = 0.3$ is close to the MPB of the $(1-x)$PZT–(x)PCN system, where the structure of the PZT–PCN compositions gradually changes from tetragonal to pseudo cubic. The electrical data described later on will further support this assumption.

The SEM images in Fig. 2 reveal that the addition of PCN resulted in significant changes in the microstructure of the ceramics. Some grains are observed to have irregular shapes with both open and close pores as a result of the high rate of the evaporation of PbO during the sintering.[17)] The images also show that the grain size of the ceramics varied considerably from 0.43 to 19.56 µm (Table I). However, the average grain size significantly decreased with an increase in the content of PCN. It can also be seen that the maximum density is obtained in the 0.7PZT–0.3PCN ceramics, while the minimum density is observed in the 0.5PZT–0.5PCN ceramics. Interestingly, the density results can be correlated to the microstructure because high-density 0.7PZT–0.3PCN ceramics show high degrees of grain close packing, whereas low-density 0.5PZT–0.5PCN ceramics contain many closed pores.

The dielectric properties of $(1-x)$PZT–(x)PCN, where $x = 0.1$–0.5, are illustrated in Fig. 3. At RT, with an increase in the concentration of PCN, the dielectric constant tends to increase because the transition temperature of the PZT–PCN ceramics shift across RT; hence, the value of the dielectric properties measured at RT increased, as shown in Table II. Other authors have reported a similar behavior.[5)] The temperature dependence of the dielectric constant for the compositions of the $(1-x)$PZT–(x)PCN system show broad dielectric peaks with an increase in the concentration of PCN, which indicate a diffuse phase transition. The diffuse phase transition may have been caused by a decrease in grain size; the observed difference in the degree of diffuseness could be a result of the grain size variation, as shown in Table II,[21)] and chemical inhomogenieties within the $(1-x)$PZT–(x)PCN solid solution.[20)]

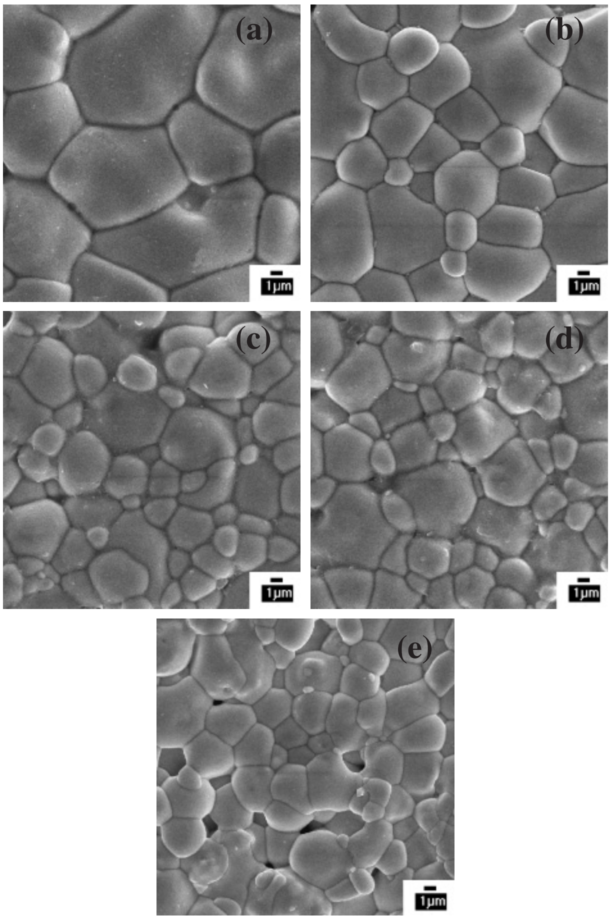

Fig. 2. SEM images of $(1-x)$PZT–(x)PCN ceramics with various compositions: $x =$ (a) 0.1, (b) 0.2, (c) 0.3, (d) 0.4, and (e) 0.5.

Table I. Physical characteristics of $(1-x)$PZT–(x)PCN ceramics, where $x = 0.1$–0.5.

Ceramics ($x = 0.1$–0.5)	Density (g/cm^3)	Grain size range (μm)	Average grain size (μm)
0.9PZT–0.1PCN	7.39 ± 0.05	4.54–19.56	7.45 ± 0.05
0.8PZT–0.2PCN	7.46 ± 0.05	2.60–12.35	4.13 ± 0.05
0.7PZT–0.3PCN	7.62 ± 0.05	0.43–9.48	2.82 ± 0.05
0.6PZT–0.4PCN	7.42 ± 0.05	0.60–10.75	2.77 ± 0.05
0.5PZT–0.5PCN	7.31 ± 0.05	0.47–9.53	2.61 ± 0.05

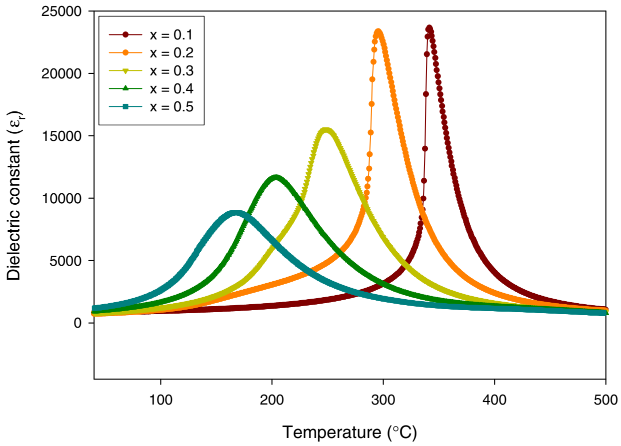

Fig. 3. (Color online) Dielectric constant (ε_r) of $(1-x)$PZT–(x)PCN ceramics at 100 kHz.

It should be noted that the formation of MPB could be clearly seen by the crystal structure analysis as described earlier. As is well known, the value of the dielectric and ferroelectric properties of a solid solution with MPB usually maximize approximately at the MPB. An anomaly at the MPB has been observed by our group in solid solution (x)PZT–$(1-x)$PNN.[5] However, no anomalies approximately at the MPB in the dielectric properties (Table II) could be found in the present work. In addition, the ferroelectric properties at approximately $x = 0.3$ are only slightly different from those of other compositions ($x = 0.2$, 0.4), rather than being “anomalously high”. This could possibly be caused by a substitution of Ni^{2+} by Co^{2+} in the B-site, which shifts the MPB composition from $x = 0.2$ in the PZT–PNN system to $0.2 \leq x \leq 0.3$ in PZT–PCN. Since in this current work, we only started with compositions at 0.1 intervals, the exact MPB composition could not be clearly identified. However, as seen in Table II, the argument that the MPB composition should fall between $0.2 \leq x \leq 0.3$ in PZT–PCN is supported by all the XRD and electrical data, which show drastic decreases in the value of the electrical properties in compositions with $x > 0.3$.

The temperature dependence of the dielectric constant (ε_r) measured at 100 kHz for the $(1-x)$PZT–(x)PCN samples with $x = 0.1$–0.5 is shown in Fig. 3. In an ideal solid solution of PZT and PCN, the transition temperature is expected to vary linearly between 341 and 167 °C. As shown in Table II, the Curie temperature decreased as expected with an increase in PCN content. However, the ε_r peaks became broader with increasing PCN content at $x \geq 0.3$. It was confirmed that the composition with $0.2 \leq x \leq 0.3$ is close to the morphotropic phase boundary (MPB) of the $(1-x)\mathrm{Pb}(\mathrm{Zr}_{1/2}\mathrm{Ti}_{1/2})\mathrm{O}_3$–$(x)\mathrm{Pb}(\mathrm{Co}_{1/3}\mathrm{Nb}_{2/3})\mathrm{O}_3$ system.

Table II. Dielectric and ferroelectric properties of $(1-x)$PZT–(x)PCN ceramics, where $x = 0.1$–0.5.

Ceramics ($x = 0.1$–0.5)	T_C (°C)	Dielectric properties				Ferroelectric properties (at 25 °C)			Loop squareness (R_{sq})
		ε_{max}	ε_{RT}	γ	δ	P_r (μC/cm^2)	P_s (μC/cm^2)	E_c (kV/cm)	
0.9PZT–0.1PCN	341.40	23700	740	1.52	14.72	2.9	4.1	8.45	1.52
0.8PZT–0.2PCN	295.50	23400	800	1.68	15.73	20.1	21.6	6.84	1.91
0.7PZT–0.3PCN	248.40	15500	840	1.81	16.55	20.9	22.6	6.92	1.94
0.6PZT–0.4PCN	203.50	11600	910	1.82	16.68	18.6	20.3	6.30	1.93
0.5PZT–0.5PCN	167.50	8900	1180	1.97	16.92	14.5	15.2	6.10	1.92

To further understand the dielectric behavior of the PZT–PCN system, the ferroelectric transition can analyzed through the Curie–Weiss relationship. For normal ferroelectrics such as PZT and PCN, above the Curie temperature, the dielectric constant follows the following equation:

$$\varepsilon = \frac{c}{T - T_0}, \tag{1}$$

where c is the Curie constant and T_0 is the Curie–Weiss temperature.[10,21,23] For a ferroelectric with a diffuse phase transition such as the PZT–PCN solid solutions, the following equation applies:

$$\frac{1}{\varepsilon} \approx (T - T_\mathrm{m})^2, \tag{2}$$

The above equation has been shown to be valid over a wide temperature range compared with the normal Curie–Weiss law [eq. (1)].[24,25] In eq. (2), T_m is the temperature at which the dielectric constant is maximum. If the local Curie temperature distribution is Gaussian, the reciprocal permittivity can be written in the form:[5,24]

$$\frac{1}{\varepsilon} = \frac{1}{\varepsilon_\mathrm{m}} + \frac{(T - T_\mathrm{m})^\gamma}{2\varepsilon_\mathrm{m}\delta^2}, \tag{3}$$

where ε_m is the maximum permittivity, γ is the diffusivity, and δ is the diffuseness parameter. For $(1-x)$PZT–(x)PCN compositions, the diffusivity (γ) and diffuseness parameter (δ) can be estimated from the slope and intercept of the dielectric data shown in Fig. 4, and tabulated in Table II.

γ and δ are both material constants depending on the composition and structure of the material.[5] γ is the expression of the degree of dielectric relaxation, while δ is used to measure the degree of diffuseness of the phase transition. In a material with a "pure" diffuse phase transition described by the Smolenskii–Isutov relation [eq. (2)], γ is expected to be 2.[26] The mean value of the diffusivity (γ) is extracted from these plots by fitting a linear equation. The values of γ vary between 1.52 and 1.97, which confirms that diffuse phase transition occurs in the PZT–PCN system. It is important to note that in perovskite ferroelectrics, it has been established that γ and δ can be affected by microstructure features, density, and grain size.[18] For PZT-rich ceramics, γ and δ increase with an increase in PCN content, confirming the diffuse phase transitions in PZT–PCN solid solutions. It is clear that the addition of PCN increases the degree of disorder in $(1-x)$PZT–(x)PCN over the compositional range $0.1 \le x \le 0.5$ with the highest degree of diffuseness exhibited in the 0.5PZT–0.5PCN composition. It should also be mentioned here that different dielectric behaviors could also be caused by grain size variation,[21] as noted in Table I.

The polarization–field (P–E) hysteresis loops of $(1-x)$PZT–(x)PCN ceramics measured at 15 kV/cm are shown in Fig. 5. A series of well-developed and mostly symmetric hysteresis loops are observed for all compositions. It is seen that the remanent polarization (P_r) varies significantly across the compositional range. However, the coercive field E_c is relatively constant, as shown in Table II. The ferroelectric parameters obtained from the P–E loops are plotted in Fig. 6. The remnant polarization (P_r) and saturated polarization (P_s) increased from $P_\mathrm{r} = 2.9\,\mu\mathrm{C/cm^2}$ and $P_\mathrm{s} = 4.1\,\mu\mathrm{C/cm^2}$ in 0.9PZT–0.1PCN to reach maximum values of $P_\mathrm{r} = 20.9\,\mu\mathrm{C/cm^2}$ and $P_\mathrm{s} = 22.6\,\mu\mathrm{C/cm^2}$ in 0.7PZT–0.3PCN. At higher PCN contents, they then drop to $P_\mathrm{r} = 14.5\,\mu\mathrm{C/cm^2}$ and $P_\mathrm{s} = 15.2\,\mu\mathrm{C/cm^2}$ in 0.5PZT–0.5PCN. However, it should be noted that the P_r ($2.9\,\mu\mathrm{C/cm^2}$) for the composition $x = 0.1$ in the present work is

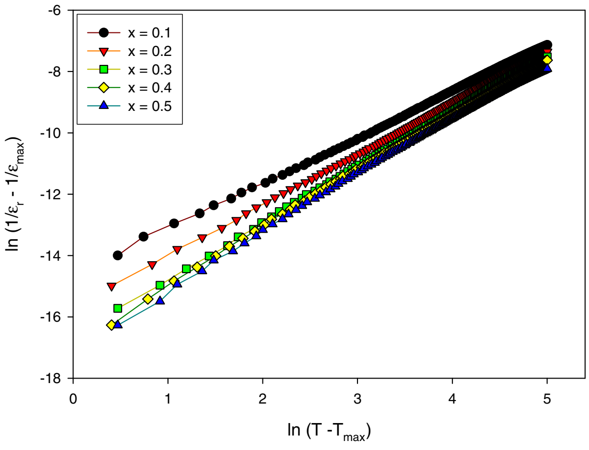

Fig. 4. (Color online) Variation of $\ln(1/\varepsilon_\mathrm{r} - 1/\varepsilon_\mathrm{max})$ vs $\ln(T - T_\mathrm{max})$ of $(1-x)$PZT–(x)PCN ceramics.

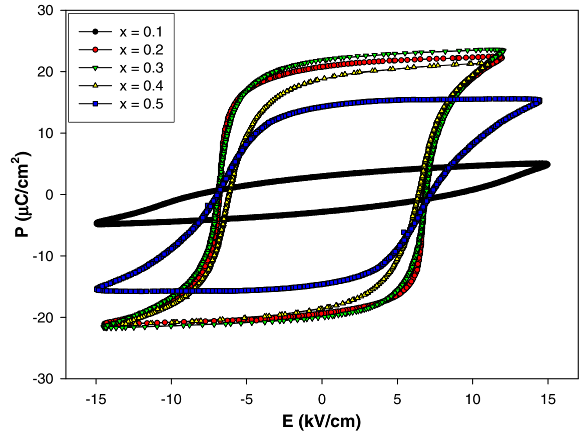

Fig. 5. (Color online) Effect of composition (x) on P–E hysteresis loops for $(1-x)$PZT–(x)PCN ceramics with $x = 0.1$–0.5.

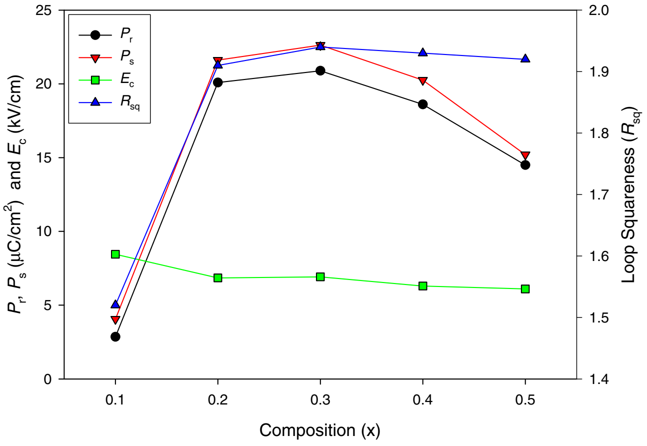

Fig. 6. (Color online) Remnant polarization (P_r), saturation polarization (P_s), coercive field (E_c), and loop squareness (R_sq) of $(1-x)$PZT–(x)PCN ceramics.

lower than the P_r ($\sim 15\,\mu C/cm^2$) in a previous study,[20] probably due to the fact that the solid-state conventional mixed oxide method used in the previous study[20] yielded two MPB compositions at $x = 0.1$ and 0.5, which is different from the columbite–wolframite method used in this study, which showed only one MPB composition at approximately $0.2 \leq x \leq 0.3$. It is well known that ferroelectric values, such as P_r, P_s, and E_c, show maximum values approximately at the MPB composition.

An empirical relationship between remnant polarization (P_r), saturation polarization (P_s) and polarization at the fields above the coercive field was derived by Haertling and Zimmer.[27] This permits the quantification of changes in the hysteresis behavior for the $(1-x)$PZT–(x)PCN samples through the following equation:

$$R_{sq} = \frac{P_r}{P_s} + \frac{P_{1.1E_c}}{P_s}, \tag{4}$$

where R_{sq} is the squareness of the hysteresis loop and $P_{1.1E_c}$ is the polarization at an electric field equal to 1.1 times the coercive field (E_c). For an ideal hysteresis loop, R_{sq} is equal to 2.0. As listed in Table II, the loop squareness parameter R_{sq} increased from 1.52 in 0.9PZT–0.1PCN to reach the maximum value of 1.94 in 0.7PZT–0.3PCN before decreasing to 1.92 in the 0.5PZT–0.5PCN composition. This observation is in good agreement with the P–E hysteresis loops, as depicted in Fig. 5. The results imply that the addition of 30 mol % PCN into PZT results in an optimized square P–E loop.

4. Conclusion

In this study, ceramics within the $(1-x)$Pb(Zr$_{1/2}$-Ti$_{1/2}$)O$_3$–(x)Pb(Co$_{1/3}$Nb$_{2/3}$)O$_3$ solid solution system (where $x = 0.1$–0.5) were successfully prepared using a solid-state mixed-oxide technique. The PZT ceramic was identified by XRD analysis as a single-phase tetragonal perovskite, while the addition of PCN resulted in a gradual shift from tetragonal symmetry to pseudo cubic symmetry, with a possible MPB between the two phases located near the 0.7PZT–0.3PCN composition. However, the dielectric and ferroelectric properties did not show anomalously high value for the dielectric and ferroelectric properties at the 0.7PZT–0.3PCN composition, indicating that the MPB composition shifted to $0.2 \leq x \leq 0.3$ in the PZT–PCN system.

Acknowledgements

This work was supported by the Commission on Higher Education (CHE), the Thailand Research Fund (TRF), the Faculty of Science, and the Graduate School of Chiang Mai University.

1) A. J. Moulson and J. M. Herbert: *Electroceramics: Materials, Properties, Applications* (Wiley, Chichester, U.K., 2003).
2) S.-E. Park and T. R. Shrout: IEEE Trans. Ultrason. Ferroelectr. Freq. Control **44** (1997) 1140.
3) J. Kuwata, K. Uchino, and S. Nomura: Ferroelectrics **37** (1981) 579.
4) M. L. Mulvihill, L. E. Cross, W. Cao, and K. Uchino: J. Am. Ceram. Soc. **80** (1997) 1462.
5) N. Vittayakorn, G. Rujijanagul, X. Tan, M. A. Marquardt, and D. P. Cann: J. Appl. Phys. **96** (2004) 5103.
6) H. Fan, G.-T. Park, J.-J. Choi, J. Ryu, and H.-E. Kim: J. Mater. Res. **17** (2002) 180.
7) O. Furukawa, Y. Yamashita, M. Harata, T. Takahashi, and K. Inagaki: *5th Meet. Ferroelectric Materials and Their Applications, Kyoto, 1985*, Jpn. J. Appl. Phys. **24** (1985) Suppl. 24-3, p. 96.
8) V. J. Tennery, K. W. Hang, and R. E. Novak: J. Am. Ceram. Soc. **51** (1968) 671.
9) D. Luff, R. Lane, K. R. Brown, and H. J. Marshallsay: Trans. J. Br. Ceram. Soc. **73** (1974) 251.
10) L. E. Cross: Mater. Chem. Phys. **43** (1996) 108.
11) G. A. Smolenskii and A. L. Agranovskaya: Sov. Phys. Tech. Phys. **3** (1958) 1380.
12) T. Kudo, T. Yazaki, F. Naito, and S. Sugaya: J. Am. Ceram. Soc. **53** (1970) 326.
13) B. A. Malkov and Y. N. Venevtsev: Izv. Akad. Nauk Neorg. Mater. **13** (1977) 1468 [in Russian].
14) V. D. Saĺniov, Y. S. Kuźminov, and Y. N. Venevtsev: Izv. Akad. Nauk Neorg. Mater. **7** (1971) 1277 [in Russian].
15) C. Xu, Z. Duan, X. Wang, D. Yang, and K. Chen: J. Cryst. Growth **281** (2005) 543.
16) N. Vittayakorn, C. Puchmark, G. Rujijanagul, X. Tan, and D. P. Cann: Curr. Appl. Phys. **6** (2006) 303.
17) N. Vittayakorn, G. Rujijanagul, T. Tankasiri, X. Tan, and D. P. Cann: Mater. Sci. Eng. B **108** (2004) 258.
18) R. Yimnirun, S. Ananta, and P. Laoratanakul: J. Eur. Ceram. Soc. **25** (2005) 3235.
19) T. Hachiga, S. Fujimoto, and N. Yasuda: J. Phys. D **20** (1987) 1291.
20) N. Vittayakorn, S. Wirunchit, S. Traisak, R. Yimnirun, and G. Rujijanagul: Curr. Appl. Phys. **8** (2008) 128.
21) R. Yimnirun, S. Ananta, and P. Laoratanakul: Mater. Sci. Eng. B **112** (2004) 79.
22) I. W. Chen, P. Li, and Y. Wang: J. Phys. Chem. Solids **57** (1996) 1525.
23) G. H. Haertling: J. Am. Ceram. Soc. **82** (1999) 797.
24) A. Halliyal, U. Kumar, R. E. Newnham, and L. E. Cross: Am. Ceram. Soc. Bull. **66** (1987) 671.
25) R. D. Shannon and C. T. Prewitt: Acta Crystallogr., Sect. B **25** (1969) 925.
26) Y.-M. Chiang, D. P. Birnie, and W. D. Kingery: *Physical Ceramics* (Wiley, Chichester, U.K., 1997) p. 522.
27) G. H. Haertling and W. J. Zimmer: Am. Ceram. Soc. Bull. **45** (1966) 1084.

Available online at www.sciencedirect.com
ScienceDirect
Ceramics International xxx (2008) xxx–xxx
CERAMICS INTERNATIONAL
www.elsevier.com/locate/ceramint

Fabrication and electrical properties of $Pb(Co_{1/3}Nb_{2/3})O_3$ ceramics

M. Unruan [a,*], N. Vittayakorn [b], R. Wongmaneerung [a], A. Prasatkhetragarn [a],
S. Ananta [a], R. Yimnirun [a]

[a] Department of Physics, Faculty of Science, Chiang Mai University, Chiang Mai 50200, Thailand
[b] Department of Chemistry, Faculty of Science, King Mongkut's Institute of Technology, Ladkrabang, Bangkok 10520, Thailand

Accepted 1 October 2007

Abstract

$Pb(Co_{1/3}Nb_{2/3})O_3$ (PCN) ceramics have been produced by sintering PCN powders synthesized from lead oxide (PbO) and cobalt niobate ($CoNb_2O_6$) with an effective method developed for minimizing the level of PbO loss during sintering. Attention has been focused on relationships between sintering conditions, phase formation, density, microstructural development, dielectric and ferroelectric properties of the sintered ceramics. From X-ray diffraction analysis, the optimum sintering temperature for the high purity PCN phase was found at approximately 1050 and 1100 °C. The densities of sintered PCN ceramics increased with increasing sintering temperature. However, it is also observed that at very high temperature the density began to decrease. PCN ceramic sintered at 1050 °C has small grain size with variation in grain shape. There is insignificant change of dielectric properties with sintering temperature. The *P–E* hysteresis loops observed at −70 °C are of slim-loop type with small remanent polarization values, which confirmed relaxor ferroelectric behavior of PCN ceramics.

Keywords: A. Sintering; C. Dielectric properties; PCN

1. Introduction

Lead-based relaxor ferroelectrics, particularly lead magnesium niobate, $Pb(Mg_{1/3}Nb_{2/3})O_3$ (PMN) belong to a technologically important class of complex $Pb(B'B'')O_3$ perovskite materials [1]. PMN has advantages of having broader operating temperature range, especially over the room temperature range. This is a direct result of a diffuse paraelectric–ferroelectric phase transition in the vicinity of room temperature. In addition, as a result of their unique microstructure features, PMN ceramics exhibit low loss and non-hysteretic characteristics [2]. However, little attention has been devoted to other lead-base relaxor ferroelectrics, $Pb(A_{1/3}B_{2/3})O_3$ (A is Mg^{2+}, Co^{2+}, Ni^{2+} or Zn^{2+} and B is Nb^{5+} or Ta^{5+}), discovered by Bokov and Myl'nikova [3], with the perovskite structure and the dielectric maximum temperature (T_m) lower than room temperature, except for that of $Pb(Zn_{1/3}Nb_{2/3})O_3$. Although Mg^{2+}, Co^{2+}, Ni^{2+} and Zn^{2+} have similar radii, the temperatures at which spontaneous polarization occurs in $Pb(A_{1/3}B_{2/3})O_3$ differ [4].

Therefore, in this study, one of lesser studied ceramics in the $Pb(A_{1/3}B_{2/3})O_3$ system, i.e. $Pb(Co_{1/3}Nb_{2/3})O_3$ (PCN), is investigated. Earlier studies have shown interesting piezoelectric properties of PCN single crystal [3]. Another study also described electrical properties of PZT-PCN ceramics [4]. However, there has been no systematic investigation on the PCN ceramics. Therefore, this study will provide more information about this interesting ceramic. Synthesis method, physical properties, microstructure, dielectric and ferroelectric properties of these ceramics are discussed.

2. Experimental procedure

PCN ceramics were prepared from starting $CoNb_2O_6$ (or CN) and PbO powders by a conventional mixed-oxide method. CN powders were obtained from the columbite method, while PCN powders were prepared by a simple mixed-oxide method. To obtain the perovskite-phase PCN, the cobalt niobate ($CoNb_2O_6$) powders were first prepared by mixing CoO (99.9%) and Nb_2O_5 (99.9%) powders in the proper proportion

---

[*] Corresponding author.
E-mail address: muangjaiunruan@yahoo.com (M. Unruan).

0272-8842/$34.00 © 2008 Elsevier Ltd and Techna Group S.r.l. All rights reserved.
doi:10.1016/j.ceramint.2007.10.033

Please cite this article in press as: M. Unruan, et al., Fabrication and electrical properties of $Pb(Co_{1/3}Nb_{2/3})O_3$ ceramics, Ceram. Int. (2008), doi:10.1016/j.ceramint.2007.10.033

and vibro-milling for 1 h. After drying, the mixtures were calcined at 1100 °C for 4 h to yield so-called columbite powders ($CoNb_2O_6$). Subsequently, the columbite powders were mixed with PbO (99.9%) by the vibro-milling method and calcined at 950 °C for 4 h to form the perovskite-phase PCN powders. Then PCN powders were pressed hydraulically to form disc-shaped pellets 8 mm in diameter and 2 mm in thickness, with 3 wt% polyvinyl alcohol as a binder. The pellets were placed in the alumina crucible. Finally, for optimization purposes, the pellets were sintered at 1050, 1100, 1150 and 1200 °C for 2 h. Optimum sintering conditions for all ceramics were established by identifying the conditions for maximizing both the bulk density and the yield of perovskite. The phase formation of the sintered ceramics was studied by X-ray diffraction (XRD) technique. The densities of sintered specimens were measured by Archimedes method. The microstructure analyses were undertaken by scanning electron microscopy (SEM: JEOL Model JSM 840A). The grain size was determined from SEM-micrographs by a linear intercept method.

Before studying the dielectric properties, the specimens were lapped to obtain parallel face. After coating with silver paint as electrode at the faces, the specimens were heated at 750 °C for 12 min to ensure contact between the electrode and the surface of the ceramic. The dielectric properties were measured by LCR-meter at temperatures between −125 and 50 °C with a frequency of 1 kHz. The dielectric constant was then calculated from a parallel-plate capacitor equation, e.g. $\varepsilon_r = Cd/\varepsilon_o A$, where C is the capacitance of the specimens, d and A are, respectively, the thickness and the area of the electrode and ε_o is the dielectric permittivity of vacuum (8.854×10^{-12} F m^{-1}). Finally, the polarization–electric field (P–E) hysteresis loops at −70 °C were obtained using a standardized ferroelectric tester system (RT66A) at a frequency of 4 Hz.

3. Results and discussion

The phase formation behavior of the sintered ceramics is revealed by an XRD method. The XRD patterns are presented in Fig. 1, with the corresponding JCPDS pattern also shown. In general, the strongest reflections apparent in the majority of the XRD patterns indicate the formation of lead cobalt niobate phases. These can be matched with JCPDS file number 04-002-0416 for the $Pb(Co_{0.33}Nb_{0.67})O_3$. Based on the JCPDS file, the optimum sintering temperature for the formation of a high purity PCN phase was found at 1050 and 1100 °C. The PCN ceramics sintered at 1150 °C showed a small peak of pyrochlore near $2\theta \sim 30°$, while the peak of PCN ceramics sintered at 1200 °C at $2\theta \sim 22°$ disappeared.

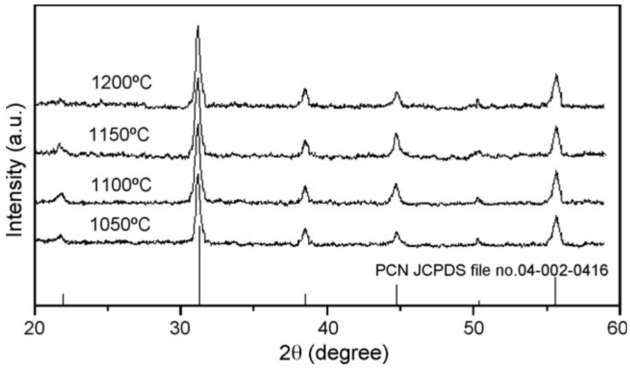

Fig. 1. XRD diffraction patterns of the sintered PCN ceramics.

Table 1
Characteristics of PCN ceramics

Sintering temperature (°C)	Relative density (%)	Average grain size (μm)	Dielectric properties	
			ε_{max}	tan δ
1050	89.39	1.83	2178	0.0594
1100	95.05	4.11	2657	0.0592
1150	95.16	6.35	2673	0.0578
1200	94.10	4.58	2248	0.0507

The relative densities of PCN ceramics sintered at different temperatures are listed in Table 1. It is clear that the density usually increases with increasing sintering temperature. This is believed to be a result of more completed solid-state reactions at higher sintering temperatures. However, it is also observed that at very high temperature the density begins to decrease. Lead-loss is generally accepted to be the reason for the decreasing density [5,6].

The SEM-micrographs of fractured surfaces of all PCN ceramics are shown in Fig. 2. PCN ceramic, sintered at 1050 °C, has small grain size with variation in grain shape. However, the other ceramics exhibit different morphology showing a possible pyrochlore formation (with pyramidal-shaped grains) and also over-sintered specimens. Table 1 also shows that the average grain size of PCN ceramics sintered at 1050 °C is relatively small, as compared to those sintered at higher temperatures. The average grain size seems to increase with increasing sintering temperatures. However, it is also observed that at very high temperature, the grain size begins to decrease, which is similar to the trend observed for the density.

Temperature dependencies of the dielectric constant (ε_r), as calculated from the capacitance of the sample and its geometry, and dielectric loss (tan δ) were measured continuously by increasing temperature from −125 to 50 °C. The temperature dependence of the dielectric constant and dielectric loss for the PCN ceramics are plotted in Fig. 3. As the measuring temperature increases, the maximum dielectric constant (ε_{max}) appear at −30 °C, this temperature is called dielectric maxima temperature (T_m). There is also insignificant change of ε_{max} with different sintering temperatures. The dielectric loss shows only very small decrease with decreasing temperature below the T_m and its value is much higher than that above the temperature of maximum dielectric constant. A strongly diffused dielectric peak is characteristic of ferroelectric relaxors. Frequency-dependent dielectric properties below T_m (not shown here) are also observed, further indicating relaxor behavior of PCN ceramics. Based on X-ray diffraction analysis, density data, SEM-micrograph, and dielectric properties, the optimum sintering temperature for a high purity PCN ceramic is found to be about 1050 and 1100 °C.

Please cite this article in press as: M. Unruan, et al., Fabrication and electrical properties of $Pb(Co_{1/3}Nb_{2/3})O_3$ ceramics, Ceram. Int. (2008), doi:10.1016/j.ceramint.2007.10.033

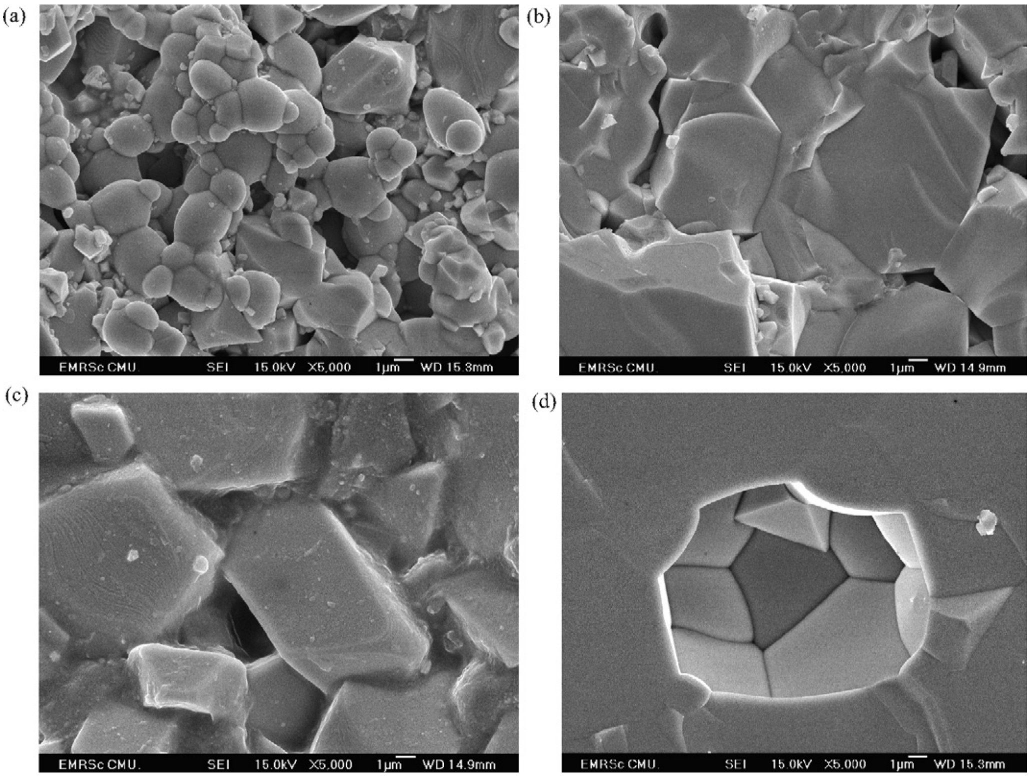

Fig. 2. SEM-micrographs of PCN ceramics at different sintering temperature: (a) 1050 °C; (b) 1100 °C; (c) 1150 °C; (d) 1200 °C.

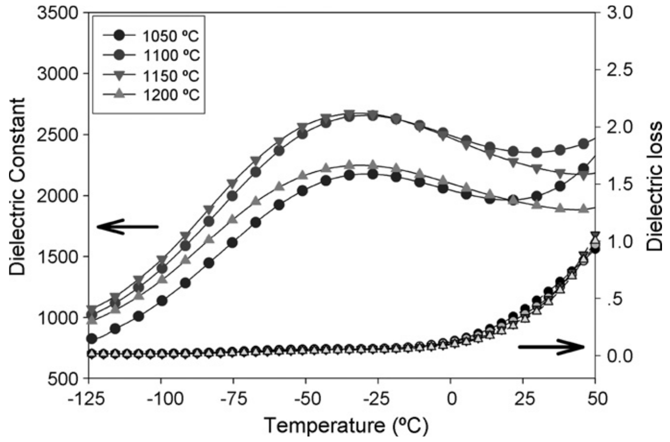

Fig. 3. Temperature dependence of dielectric properties of PCN ceramics at 1 kHz.

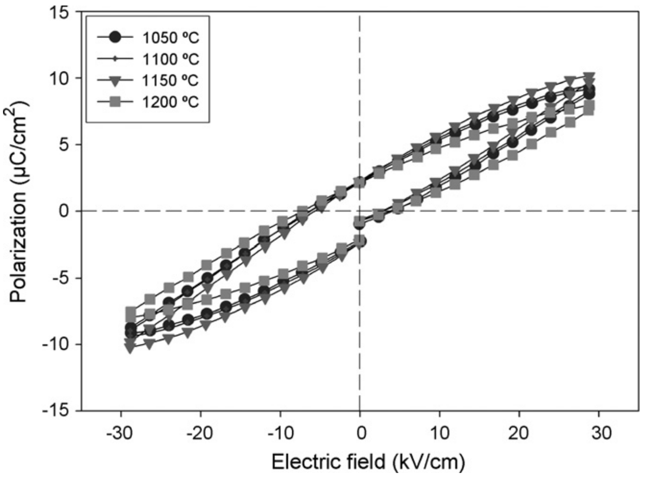

Fig. 4. *P–E* hysteresis loops of PCN ceramics measured at −70 °C and frequency 50 Hz.

The hysteresis loops at −70 °C of PCN ceramics sintered at different temperatures are shown in Fig. 4. It can be seen that slim *P–E* loops with small remanent polarization values are generally obtained for all ceramics. The slim-loop nature of the *P–E* curves suggests that most of the aligned dipole moments switch back to a randomly oriented state upon removal of the field. This behavior has previously been observed in ferroelectric relaxors [7]. In relaxor ferroelectric materials, micro to macro-domain transition occurs. In the absence of any external field, the domain structure of relaxor ferroelectrics contains randomly oriented micropolar regions. However, when an electric field is applied, the micro-domains orient along the field direction and the macro-domains occur [7]. The *P–E* loops observed here also support that the PCN ceramics exhibit relaxor ferroelectric behavior.

4. Conclusions

In this study, PCN ceramics were prepared by the columbite precursor method. The PCN ceramics with perovskite structure and a high purity single phase were obtained. The optimum

Please cite this article in press as: M. Unruan, et al., Fabrication and electrical properties of $Pb(Co_{1/3}Nb_{2/3})O_3$ ceramics, Ceram. Int. (2008), doi:10.1016/j.ceramint.2007.10.033

sintering temperature for the formation of a high purity PCN phase was found to be at 1050 and 1100 °C. Density of these ceramics increases with increasing sintering temperature. However, at very high temperature the density begins to decrease. There is insignificant change of dielectric properties with different sintering temperatures. The samples exhibit a relaxor behavior around the maximum dielectric constant, characterized by a strongly diffused dielectric peak. The hysteresis loops at −70 °C show slim *P–E* loops with small remanent polarization values. This behavior has been observed in ferroelectric relaxors.

Acknowledgements

This work is supported by the Thailand Research Fund (TRF), Commission on Higher Education (CHE), and Royal Golden Jubilee (RGJ) Ph.D. Program. Additional supports from the Faculty of Science and Graduate School of Chiang Mai University are gratefully acknowledged.

References

[1] K. Vladimir, B. Jaroslav, Microstructure and electrical response of $0.9Pb(Mg_{1/3}Nb_{2/3})O_3$-$0.1PbTiO_3$ relaxor ceramics, Ceramics-Silikaty 47 (1) (2003) 8–12.

[2] L.E. Cross, Relaxor ferroelectrics, Ferroelectric 76 (1987) 241–267.

[3] V.A. Bokov, I.E. Myl'nikova, Piezoelectric properties of new compound single crystal with perovskite structure, Fiz. Tverd. Tela 2 (11) (1960) 2728–2732.

[4] T. Kudo, T. Yazaki, F. Naito, S. Sugaya, Dielectric and piezoelectric properties of $Pb(Co_{1/3}Nb_{2/3})O_3$-$PbTiO_3$-$PbZrO_3$ solid solution ceramics, J. Am. Ceram. Soc. 53 (1969) 326–328.

[5] V. Koval, C. Alemany, J. Briancin, H. Brunckova, K. Saksl, Effects of PMN modification of structure and electrical response of xPMN-(1-x)PZT ceramic systems, J. Eur. Ceram. Soc. 23 (2003) 1157–1166.

[6] J.H. Park, K.H. Yoon, D.H. Kang., Dielectric and electrical properties of preferentially (111) oriented Zr-rich $0.1Pb(Mg_{1/3}Nb_{2/3})O_3$-$0.9Pb(Zr_xTi_{1-x})O_3$ thin films by chemical solution deposition, Thin Solid Films 396 (2001) 84–89.

[7] A. Peláiz-Barranco, I. González-Carmenate, F. Calderón-Piñar, Relaxor behavior in PZN–PT–BT ferroelectric ceramics, Solid State Commun. 134 (2005) 519–522.

Please cite this article in press as: M. Unruan, et al., Fabrication and electrical properties of $Pb(Co_{1/3}Nb_{2/3})O_3$ ceramics, Ceram. Int. (2008), doi:10.1016/j.ceramint.2007.10.033

ELSEVIER
Journal of Alloys and Compounds xxx (2007) xxx–xxx
Journal of ALLOYS AND COMPOUNDS
www.elsevier.com/locate/jallcom

Synthesis and properties of $Pb(Co_{1/3}Nb_{2/3})O_3$ ceramics

Muangjai Unruan [a], Naratip Vittayakorn [b], Rewadee Wongmaneeruang [a], Anurak Prasatkhetragarn [a], Supon Ananta [a], Rattikorn Yimnirun [a,*]

[a] *Department of Physics, Faculty of Science, Chiang Mai University, Chiang Mai 50200, Thailand*
[b] *Department of Chemistry, Faculty of Science, King Mongkut's Institute of Technology Ladkrabang, Bangkok 10520, Thailand*

Received 7 June 2007; received in revised form 3 November 2007; accepted 11 November 2007

Abstract

In this study, $Pb(Co_{1/3}Nb_{2/3})O_3$ or PCN ceramics have been produced by sintering PCN powders synthesized from lead oxide (PbO) and cobalt niobate ($CoNb_2O_6$) with an effective method developed for minimizing the level of PbO loss during sintering. Attention has been focused on relationships between sintering conditions, phase formation, density, microstructural development, dielectric and ferroelectric properties of the sintered ceramics. The densities of sintered PCN ceramics increased with increasing sintering temperature. However, it was observed that at too high temperature the density began to decrease. Change of dielectric properties with sintering temperature also followed the same trend as the density. Based on X-ray diffraction analysis, density data, SEM micrograph, and dielectric properties, the optimum sintering temperature for a high purity PCN ceramic was found to be about 1100 and 1150 °C. A strongly diffused dielectric peak also showed a typical characteristic of ferroelectric relaxors. The P–E hysteresis loops observed at −70 °C were of slim-loop type with small remnant polarization values, which confirmed relaxor ferroelectric behavior of PCN ceramics.

Keywords: Dielectric properties; Sintering; PCN

---

1. Introduction

Lead-base relaxor ferroelectrics, particularly lead magnesium niobate, $Pb(Mg_{1/3}Nb_{2/3})O_3$ (PMN) belong to a technologically important class of complex $Pb(B'B'')O_3$ perovskite materials [1]. PMN has advantages of having broader operating temperature rang, especially over the room temperature rang. This is a direct result of a diffuse paraelectric–ferroelectric phase transition in the vicinity of room temperature. In addition, as a result of their unique microstructure features PMN ceramics exhibit low loss and non-hysteretic characteristics [2]. However, little attention has been devoted to the other lead-base relaxor ferroelectrics, $Pb(A_{1/3}B_{2/3})O_3$ (A is Mg^{2+}, Co^{2+}, Ni^{2+} or Zn^{2+} and B is Nb^{5+} or Ta^{5+}), discovered by Bokov and Mylnikova [3], with the perovskite structure and the dielectric maxima temperature (T_m) lower than room temperature except for that of $Pb(Zn_{1/3}Nb_{2/3})O_3$. Although Mg^{2+}, Co^{2+}, Ni^{2+} and Zn^{2+} have similar radii, the temperatures at which spontaneous polarization occurs in $Pb(A_{1/3}B_{2/3})O_3$ differ [4].

Therefore, in this study one of lesser studied ceramics in the $Pb(A_{1/3}B_{2/3})O_3$ system, i.e. $Pb(Co_{1/3}Nb_{2/3})O_3$ (PCN) is investigated. Synthesis method, physical properties, microstructure, dielectric and ferroelectric properties of the ceramic are discussed.

2. Experimental method

PCN ceramics were prepared from starting PbO and $CoNb_2O_6$ (or CN) powders by a conventional mixed oxide method. CN powders were obtained from the columbite method [5], while PCN powders were prepared by a simple mixed oxide method. To obtain the perovskite-phase PCN, the cobalt niobate ($CoNb_2O_6$) powders were first prepared by mixing CoO (99.9%) and Nb_2O_5 (99.9%) powders in the proper proportion and vibro-milling for 1 h. After drying, the mixtures were calcined at 1100 °C for 4 h to yield so-called columbite powders ($CoNb_2O_6$). Subsequently, the columbite powders were mixed with PbO (99.9%) by the vibro-milling method and calcined at 950 °C for 4 h to form the perovskite-phase PCN powders. Then PCN powders were pressed hydraulically to form disc-shaped pellets 8 mm in diameter and 2 mm thick, with 3 wt% polyvinyl alcohol as a binder. The pellets were placed in the alumina crucible. Finally, for optimization purposes the pellets were sintered at 1050, 1100, 1150 and 1200 °C for 2 h. The phase formation of the sintered ceramics was studied by the X-ray diffraction (XRD) technique. The densities of sintered spec-

---

* Corresponding author. Tel.: +66 53 943 367; fax: +66 53 943 445.
E-mail address: rattikornyimnirun@yahoo.com (R. Yimnirun).

0925-8388/$ – see front matter © 2007 Elsevier B.V. All rights reserved.
doi:10.1016/j.jallcom.2007.11.071

Please cite this article in press as: M. Unruan, et al., J. Alloys Compd. (2007), doi:10.1016/j.jallcom.2007.11.071

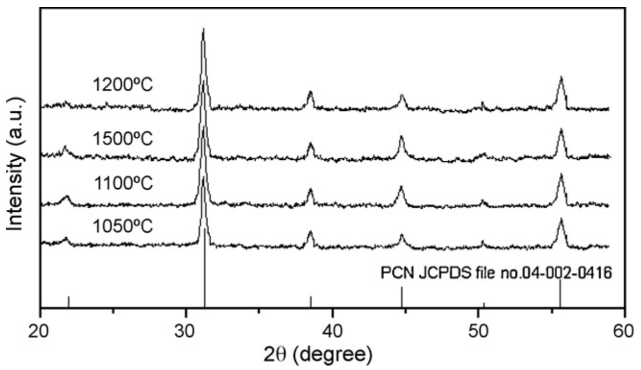

Fig. 1. XRD diffraction patterns of the sintered PCN ceramics.

imens were measured by Archimedes method. The microstructure analyses were undertaken by scanning electron microscopy (SEM: JEOL Model JSM 840A). The grain size was determined from SEM micrographs by a linear intercept method.

Before studying the dielectric properties, the specimens were lapped to obtain parallel faces. After coating with silver paint as electrode on the faces, the specimens were heated at 750 °C for 12 min to ensure contact between the electrode and the surface of the ceramic. The dielectric properties (dielectric constant (ε_r) and dielectric loss ($\tan\delta$)) were measured at temperatures between −120 and 50 °C. The capacitance was measured with a HP4284A LCR meter in connection with a Delta Design 9023 temperature chamber and a sample holder (Norwegian Electroceramics). The dielectric constant (ε_r) was then calculated from a parallel-plate capacitor equation, e.g. $\varepsilon_r = Cd/\varepsilon_o A$, where C is the capacitance of the specimens, d and A are, respectively, the thickness and the area of the electrode and ε_o is the dielectric permittivity of vacuum (8.854×10^{-12} Fm^{-1}). Finally, the polarization–electric field (P–E) hysteresis loops at −70 °C were obtained using a standardized ferroelectric tester system (RT66A) with driving frequency of 4 Hz.

3. Results and discussion

The phase formation behavior of the sintered ceramics is revealed by an XRD method. The XRD patterns are presented in Fig. 1, with the corresponding JCPDS pattern also shown. In general, the strongest reflections apparent in the majority of the XRD patterns indicate the formation of perovskite lead cobalt niobate phase. These can be matched with JCPDS file number 04-002-0416 for the $Pb(Co_{0.33}Nb_{0.67})O_3$. Based on the XRD analysis, the optimum sintering temperature for the formation of a high purity PCN phase was found at 1100 °C.

The densities of PCN ceramics sintered at different temperatures are listed in Table 1. It is clear that the density usually increases with increasing sintering temperature. This is believed to be a result of more completed solid-state reactions at higher sintering temperatures. However, it is also observed that at too high temperature the density begins to decrease. Lead-loss is generally accepted to be the reason for the decreasing density [6].

The SEM micrographs of fractured surfaces of all PCN ceramics are shown in Fig. 2. PCN ceramic sintered at 1050 °C has small grain size with variation in grain shape. However, the other ceramics exhibit different morphology showing a possible pyrochlore formation (with pyramidal-shaped grains) and also over-sintered specimens. Table 1 also shows that the average grain size of PCN ceramics sintered at 1050 °C is relatively small, as compared to those sintered at higher temperatures. The average grain size increases with increasing sintering temperatures. However, it is also observed that at very high temperature the grain size begins to decrease, which is similar to the trend observed for the density. Change of dielectric properties with sintering temperature also followed the same trend as the density. The dielectric constant reaches maximum values at sintering temperature of 1150 °C.

Temperature and frequency dependencies of ε_r, as calculated from the capacitance of the sample and its geometry, and $\tan\delta$ were measured continuously by increasing temperature from −120 to 50 °C and frequency rang from 100 Hz to 100 kHz. The temperature dependence of ε_r and $\tan\delta$ for the PCN ceramics are plotted in Fig. 3. As the measuring temperature increases the maximum dielectric constant (ε_{max}) appears at −30 °C, this temperature is called dielectric maxima temperature (T_m). It should be noticed that T_m obtained in this study is different from previous studies [3,7–9], which reported T_m of −70 °C for single crystal PCN and stress-dependent T_m for PCN ceramics ranging from −20 to −50 °C. It could be said that the T_m values obtained in this study fall within the previously reported values. This is because in this current study the dielectric properties, which are used to determine T_m, of the PCN ceramic were measured under compressive stress from a rather heavy sample holder used in the measurement system. In addition, the ceramics may also contain internal residual stress. Therefore, the T_m values obtained in this study are slightly lower than the previously reported value under stress-free condition. There is also insignificant change of T_m with different sintering temperatures. The $\tan\delta$ shows only very small decrease with decreasing temperature below the T_m and $\tan\delta$ becomes very high above the temperature of maximum dielectric constant. Based on X-ray diffraction analysis, density data, SEM micrograph, and dielectric properties, the optimum sintering

Table 1
Characteristics of PCN ceramics

Sintering temperature (°C)	Density (g/cm^3)	Average grain size (μm)	Dielectric properties	
			ε_{max}	$\tan\delta$
1050	7.58	1.83	2178	0.0594
1100	8.06	4.11	2657	0.0592
1150	8.07	6.35	2673	0.0578
1200	7.98	4.58	2248	0.0507

Please cite this article in press as: M. Unruan, et al., J. Alloys Compd. (2007), doi:10.1016/j.jallcom.2007.11.071

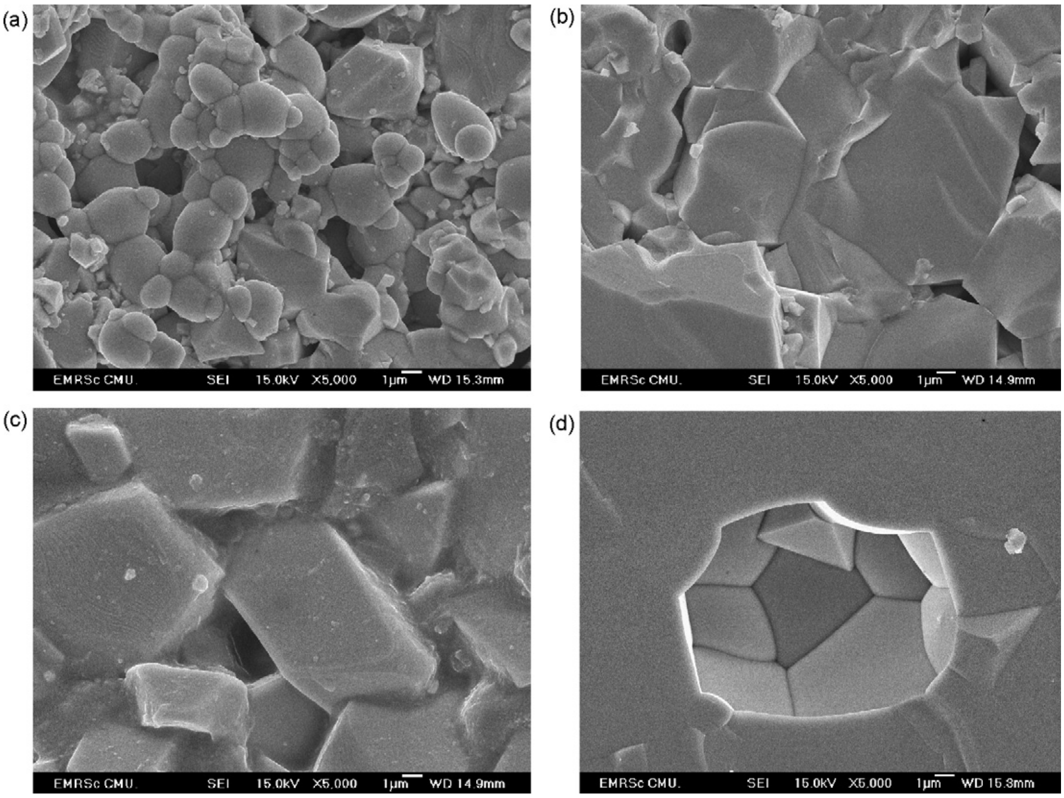

Fig. 2. SEM micrographs of PCN ceramics at different sintering temperature: (a) 1050 °C; (b) 1100 °C; (c) 1150 °C; and (d) 1200 °C.

temperature for a high purity PCN ceramic is found to be about 1100 and 1150 °C.

A strongly diffused dielectric peak is characteristic of ferroelectric relaxors. Frequency-dependent dielectric properties below T_m are also observed (Fig. 4.), further indicating relaxor behavior of PCN ceramics. However, one would expect to see a strong shift in T_m with frequency, as expected for typical relaxors, such behavior is not clearly visible because very high tan δ above T_m causes ε_r to increase rapidly.

The hysteresis loops at −70 °C of PCN ceramics sintered at different temperatures are shown in Fig. 5. It can be seen that slim P–E loops with small remnant polarization values are generally obtained for all ceramics. The slim-loop nature of the P–E curves suggests that most of the aligned dipole moments switch back to a randomly oriented state upon removal of the field. This behavior has previously been observed in ferroelectric relaxors [10]. In relaxor ferroelectric materials, micro- to macro-domain transition occurs. In the absence of any external field, the domain structure of relaxor ferroelectrics contains randomly oriented micropolar regions. However, when an electric field is applied, the micro-domains orient along the field direction and the macro-domains occur [10]. The P–E loops observed here also support that the PCN ceramics exhibit relaxor ferroelectric behavior.

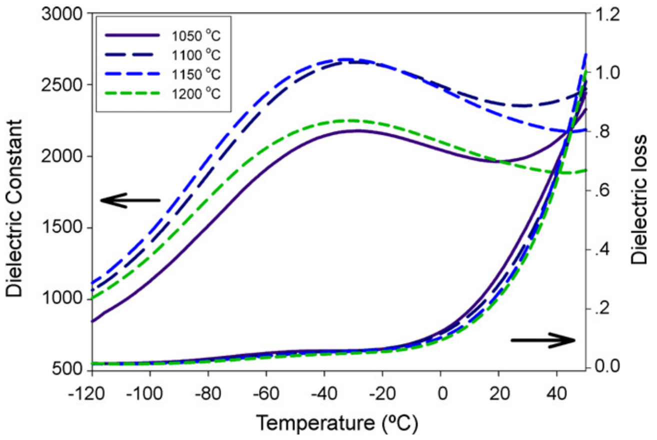

Fig. 3. Temperature dependence of dielectric properties of PCN ceramics at 1 kHz.

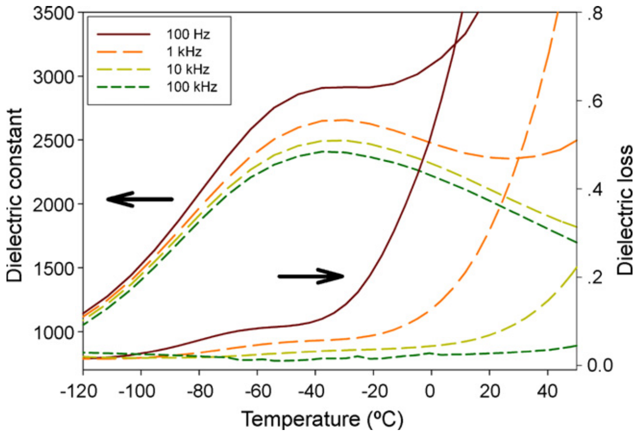

Fig. 4. Temperature and frequency dependence of dielectric properties of PCN ceramic sintered at 1100 °C.

Please cite this article in press as: M. Unruan, et al., J. Alloys Compd. (2007), doi:10.1016/j.jallcom.2007.11.071

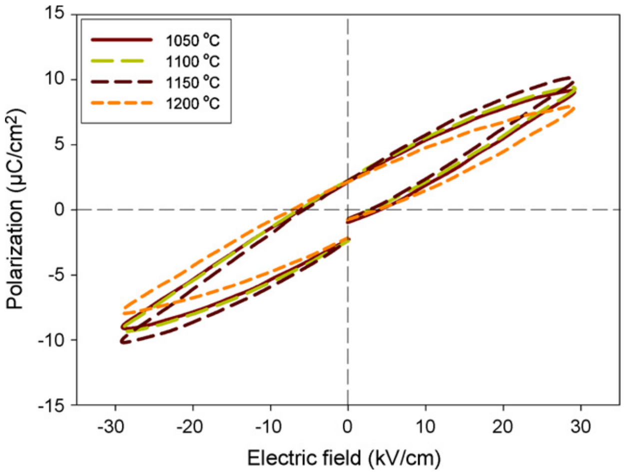

Fig. 5. P–E hysteresis loops of PCN ceramics measured at −70 °C (4 Hz).

4. Conclusions

In this study, PCN ceramics were prepared by the columbite precursor method. The PCN ceramics with perovskite structure and a high purity single phase are obtained. Density of these ceramics increases with increasing sintering temperature. However, at too high temperature the density begins to decrease. Change of dielectric properties with sintering temperature also follows the same trend as the density. Based on X-ray diffraction analysis, density data, SEM micrograph, and dielectric properties, the optimum sintering temperature for a high purity PCN ceramic is found to be about 1100 and 1150 °C. The samples exhibit a relaxor behavior around the maximum dielectric constant, characterized by a strongly diffused dielectric peak at −30 °C. The hysteresis loops measured at −70 °C show slim P–E loops with small remnant polarization values. This behavior has been observed in ferroelectric relaxors.

Acknowledgments

This work is supported by the Thailand Research Fund (TRF) and Commission on Higher Education (CHE). Additional supports from the Faculty of Science and Graduate School of Chiang Mai University are gratefully acknowledged.

References

[1] K. Vladimir, B. Jaroslav, Ceramics-Silikaty 47 (2003) 8.
[2] L.E. Cross, Ferroelectrics 76 (1987) 241.
[3] V.A. Bokov, I.E. Mylnikova, Sov. Phys. Solid State (Eng. Transl.) 2 (1961) 2428.
[4] T. Kudo, T. Yazaki, F. Naito, S. Sugaya, J. Am. Ceram. Soc. 53 (1969) 326.
[5] S.L. Swartz, T.R. Shrout, Mater. Res. Bull. 17 (1982) 1245.
[6] R. Yimnirun, S. Ananta, P. Laoratanakul, J. Eur. Ceram. Soc. 25 (2005) 3225.
[7] Landolt-Bornstein, in: T. Mitsui, S. Nomura (Eds.), Ferroelectrics and Related Substances, vol. 16, Springer-Verlag, Berlin, 1981.
[8] Y. Yamashita, Jpn. J. Appl. Phys. 33 (1994) 5328.
[9] T. Huchiga, S. Fujimoto, N. Yasuda, J. Phys. D: Appl. Phys. 20 (1987) 1291.
[10] A. Peláiz-Barranco, I. González-Carmenate, F. Calderón-Piñar, Solid State Commun. 134 (2005) 519–522.

Please cite this article in press as: M. Unruan, et al., J. Alloys Compd. (2007), doi:10.1016/j.jallcom.2007.11.071